Data Efficient Solar Disaggregation with Behind-the-meter Energy Resources

by

Xinlei Chen

A thesis submitted in partial fulfillment of the requirements for the degree of

Master of Science

Department of Computing Science

University of Alberta

Abstract

Solar photovoltaic (PV) generation is one of the fastest-growing renewable energy sources worldwide. Almost half of this growth is projected to be behind-the-meter (BTM) installations – typically PV systems mounted on the rooftop of a home or a commercial building. Today, utilities neither have visibility into BTM distributed energy resources (DER) nor the analytical tools to reliably estimate the amount of solar power injected at any given time into their distribution feeders, a vital piece of information for crafting new tariffs and planning future investments to mitigate voltage problems and manage bidirectional power flows. This has given rise to research on signal processing and machine learning techniques that can be applied to disaggregate solar generation from the net load that is measured by a smart meter. In addition, as battery pack prices continue to decline and new pricing schemes are being introduced, many customers with PV installations will be inclined to install a battery to shift the PV output to align with the peak demand time. This "solar-plus-battery" system, when installed behind the meter, makes the disaggregation problem even harder to solve because some fluctuations in the net load that were useful for disaggregation will be smoothed out by the battery. This thesis aims to solve some of the challenges in the solar disaggregation problem under the assumption that the historical disaggregated data from the target home is unavailable and the deployment characteristic of BTM energy resources (e.g., PV systems and batteries) are unknown. We propose a data-efficient solar disaggregation method to estimate solar power generated

by a BTM PV system and show that as long as there is one real proxy, other real proxies can be replaced with synthetic ones generated by a physical PV model with negligible loss of accuracy. We then examine how the improved solar disaggregation accuracy affects the performance of three state-of-the-art non-intrusive load monitoring (NILM) methods, namely Factorial Hidden Markov Model (FHMM), Sequence-to-Point (Seq2Point), and Denoising Autoencoder (DAE). NILM methods help residential customers understand how much money they spend on different appliances, especially energy-hungry appliances, such as air conditioner and furnace. Finally, we extend our solar disaggregation method by considering BTM battery storage. We discuss how the physical characteristics of the battery can be inferred from net meter data and how they can be used to facilitate disaggregation. Using a real dataset, we compare our methods with several state-of-the-art methods in two scenarios, which include customers with and without a BTM battery, and show that our methods outperform baselines by a clear margin.

Preface

This thesis is original work by Xinlei Chen. Some of the chapters are based on conference papers that are co-authored by the author of this thesis.

Specifically, Parts of Chapter 2 were published as a workshop paper: Xinlei Chen and Omid Ardakanian. 2020. "Solar Disaggregation: State of the Art and Open Challenges", in Proceedings of the 5th International Workshop on Non-Intrusive Load Monitoring (NILM'20). As the first author, I was responsible for reviewing the literature, and identifying existing challenges and opportunities.

Chapter 3 appeared in the following conference paper: Xinlei Chen, Moosa Moghimi Haji, and Omid Ardakanian. 2021. "Disaggregating Solar Generation Using Smart Meter Data and Proxy Measurements from Neighbouring Sites", in Proceedings of the Twelfth ACM International Conference on Future Energy Systems (e-Energy '21). I was responsible for doing part of the literature review, developing the methodology, running experiments, and producing results and figures. Moosa Moghimi Haji provided advice on the methodology design, contributed to the writing of the introduction and literature review, and helped with editing the manuscript. Chapter 4 has been recently submitted to *IEEE Transactions on Smart Grid* and is currently under review. The authors are me and Dr. Omid Ardakanian. I was responsible for reviewing literature, developing the methodology, running experiments, and producing results.

For all of the above mentioned papers, my supervisor, Dr. Omid Ardakanian, edited the manuscript and provided excellent guidance and supervision.

Wonder is the beginning of wisdom.

– Socrates, Philosopher.

Acknowledgements

The person I would most like to thank is my supervisor Dr. Omid Ardakanian. Joining his research group has really helped me find the direction I want to pursue in the future. I would not have been able to complete my research and thesis without his help and guidance. I am also very grateful for his help and encouragement when things were not going well during my graduate studies.

Special thanks to Dr. Moosa Moghimi Haji for his help and advice during my research work.

Finally, I would also like to thank my friends and family for their endless support.

Contents

List of Tables

List of Figures

Chapter 1

Introduction

In the past few decades, substantial changes have occurred in the traditional grid. These changes were primarily driven by the integration of demand-side technologies, such as distributed energy resources (DER) and controlled loads, into low-voltage distribution networks, aiming to improve its efficiency and reduce carbon emissions [1]. Solar photovoltaic (PV) is one of the most widely used renewable technologies, which is currently enjoying the fastest growth rate among renewable sources worldwide thanks to declining costs of solar projects and government tax credits. Solar PV generation in end-use sectors in the U.S. is anticipated to increase more than fourfold, from 41 billion kilowatt-hours (1% of U.S. generation) to 182 billion kilowatt-hours (4% of U.S. generation) by 2050 [18].

The large-scale adoption of distributed PV systems and the rising number of prosumers (i.e., energy producers and consumers) present new challenges for planning and operation of power distribution grids, from the management of voltage to the configuration of protection systems and increased wear and tear on utility equipment. In light of this, utility companies seek innovative solutions to identify unregistered solar panels, and estimate their peak capacity and real-time production. Since most distributed PV systems will be installed behind the meter (BTM) [25], the most reliable and effective method is to install additional sensors to measure the solar generation of each BTM PV system directly. However, this is not only costly, but also raises privacy concerns. For example, it has been shown in [10] that it is possible to localize

"anonymous" solar-powered homes using their solar generation data only.

In the past few years, millions of smart meters have been rolled out around the world to collect high resolution data from customers. One potential low-cost and less-intrusive approach to estimate solar generation by BTM PV systems is to develop methods that only rely on the data that is commonly available to electric utilities, in particular, weather information and net meter data (i.e., home load minus solar generation) from advanced metering infrastructure (AMI). In fewer cases, substation-level and feeder-level voltage and current phasor measurements from the supervisory control and data acquisition system (SCADA) or distribution-level phasor measurement units (D-PMUs) [39] can also be utilized.

1.1 Identification of BTM solar PV systems

Several methods have been proposed in the literature to estimate the solar power generated by BTM PV systems. They can be divided into three major categories:

(a) Methods that rely on satellite and aerial imagery [21] to identify PV systems and estimate their physical characteristics, e.g., size, tilt, and orientation. These approaches provide a rough estimate of the peak production capacity, but cannot accurately estimate solar generation at a given time.

(b) Methods that rely on a few separately metered solar sites in a geographical area to estimate the total solar generation in that area [46], [47]. These methods require knowledge of the total installed capacity of PV systems in the area, which is not available in many cases.

(c) Methods that apply signal separation techniques to disaggregate solar generation from feeder-level measurement or smart meter data [9], [13]. The main advantage of the *solar disaggregation* methods that only require smart meter data is that they are widely applicable as they do not require additional information.

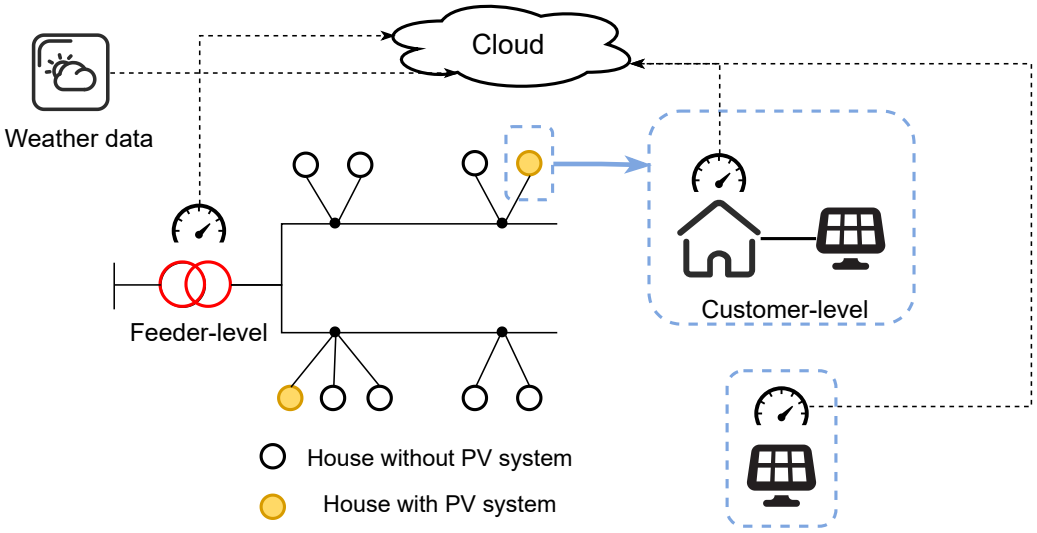

Figure 1.1: The overview of customer-level and feeder-level solar disaggregation.

1.2 Solar disaggregation

Solar disaggregation is the problem of estimating solar generation from net load measurements which can be obtained at different levels of aggregation. Customer-level solar disaggregation is to separate the power consumption measured by a smart meter into household (or business) demand and solar generation. Feeder-level (or substation-level) solar disaggregation concerns separating the overall solar generation at the feeder from the total active power consumption of loads connected to that feeder. Figure 1.1 shows the similarities and differences between customer-level and feeder-level solar disaggregation at a high level. Compared to other methods of estimating BTM solar generation, solar disaggregation methods only rely on the data that is commonly available to the utilities, in particular weather information and net meter data from advanced metering infrastructure with time resolutions in the range of one minute to one hour [11]. In this thesis, we focus on investigating customer-level solar disaggregation methods using net meter data collected by smart meters.

1.2.1 Differences with Non-Intrusive Load Monitoring

Solar disaggregation is closely related to non-intrusive load monitoring (NILM) [20], the problem of separating a household's total energy consumption, measured by a single meter, into individual appliance consumption data. Several techniques have been proven to be effective in NILM problem, which includes hidden Markov models (HMM) [32], deep learning [31], combinatorial optimisation (CO) [20], etc. Despite the apparent analogy between the two problems, NILM methods cannot be directly applied to separate solar generation from net load. This is partly because most NILM methods assume that the operation of each appliance can be divided into a finite number of operating states (e.g., ON, OFF, standby), and that the power consumption in each state is known and constant. Solar generation however changes continuously depending on several factors, such as solar radiation and temperature, and can have abrupt changes due to the effect of passing clouds. This diminishes the efficacy of NILM methods [15].

1.2.2 Challenges in solar disaggregation from net meter data

Despite the growing literature on solar disaggregation, there are still several key challenges, ranging from the lack of fine-grained data and an evaluation toolkit to the presence of latent components (e.g., BTM battery system and electric vehicle chargers), which hinder the application of these methods in practice. Since historical (disaggregated) data regarding solar generation and home load may not be available from a customer with a BTM PV system, the problem should be solved in an unsupervised fashion. Furthermore, the increased BTM solar penetration brings in new challenges for NILM as the smart meter reading may not be equal to the sum of the power demand of individual appliances in the daytime. This highlights the importance of disaggregating solar power from net meter data before trying to separate the household demand into the constituent appliances, and calls for incorporating solar disaggregation algorithms in NILM software, such as NILMTK [4].

In Section 2.4 and Section 2.5, we elaborate on the open challenges in this area and put forward recommendations to address them in future work. These challenges underline the scope for developing new techniques for solar disaggregation and justify the effort to collect data from a larger set of solar installations where solar generation can be separately metered.

1.2.3 Enabling NILM

Although NILM problem has been extensively studied in decades, the majority of NILM methods assume that the net load is simply the total power consumed by home appliances. As more and more households choose to install their own PV systems, those 'negative' load (i.e., solar generation) generated from PV panels may confuses many NILM methods, since solar generation is subtracted from the home load, whereas appliance loads are summed to construct the home load. Thus, it is necessary to develop reliable solar disaggregation methods to decompose the net load data into solar generation and home load. The NILM methods can then be applied to the latter component to identify the energy consumption of different appliances.

1.2.4 Dealing with BTM solar-plus-battery systems

As battery pack prices continue to decline and new pricing schemes are being introduced [41], customers with PV systems will be inclined to install a battery to shift the PV output to align with the peak demand time. This "solar-plus-battery" system, when installed behind the meter, makes the disaggregation problem even harder to solve because some fluctuations in the net load that are useful for disaggregation will be smoothed out by the battery. This calls for new disaggregation techniques that (a) rely on the data that is commonly available to utilities, e.g., weather data and smart meter readings with time resolutions in the range of 1 minute to 1 hour, and (b) maintain a high level of accuracy even when other DER, with unknown characteristics, are installed behind the meter. While extensive research has been done on disaggregating solar generation from feeder-level or building-level measurements [9], [13], [26],

[27], [35], most related work addresses this problem without considering the effect of a BTM battery.

In Chapter 4, we advance the state of the art by proposing a solar disaggregation method to accurately decompose the net load to major types of load, i.e., aggregate home load, solar generation, and power contribution of the battery when it is present.

1.3 Summary of contributions

In this thesis, we initially conduct a detailed survey of related work on solar disaggregation, and identify key challenges and research opportunities. Then, we propose two solar disaggregation methods in order to answer following three questions that arose from the survey,

- RQ1: Since the solar disaggregation problem has to be solved in an unsupervised fashion, state-of-the-art methods use measurements from a large number of neighboring PV systems to estimate solar generation of the target home. However, measurements from many PV systems in the same area may not be available in practice. So how can we disaggregate solar generation in a more data efficient way?

- RQ2: What is the accuracy of standard NILM techniques when they are applied to the disaggregated home load? Can we still understand which appliances are turned on and when?

- RQ3: How can we maintain the performance of solar disaggregation methods in the presence of BTM battery energy storage?

To address RQ1, we propose a method that has two key advantages over prior work. First, it requires active power measurements with low temporal resolution and solar generation measurements from only one or a few PV systems located in the same geographical area. Second, our method has a low computational overhead, making it suitable for large-scale implementation. To address RQ2, we apply 3 benchmark NILM techniques that are implemented in

an open source toolkit to the disaggregated home load obtained by our method. We then discuss the disaggregation result for 7 appliances that are present in most homes. To address RQ3, we extend our disaggregation method to tackle the problem in the presence of BTM battery without knowing its capacity, peak power, and control strategy.

The main contributions of this thesis are as follows:

- We propose a data-efficient disaggregation method to estimate solar power generated by a BTM PV system with unknown deployment characteristics. We show that as long as there is one real solar proxy, other real proxies can be replaced with synthetic ones that are generated by a physical PV model with negligible loss of accuracy. Comparing against two state-of-the-art solar disaggregation methods on a publicly available dataset, we find that the proposed method outperforms them in terms of the disaggregation accuracy.

- We examine how the improved accuracy of solar disaggregation affects the accuracy of three baseline NILM methods, namely Factorial Hidden Markov Model (FHMM) [19], Sequence-to-Point (Seq2Point) [61], and Denoising Autoencoder (DAE) [31]. The evaluation is done on a real dataset.

- We extend our solar disaggregation method by considering BTM battery storage. We discuss how the power rating of the battery can be inferred from net meter data and used to facilitate disaggregation. In the experiments, we use a real dataset and compare our method with one state-of-the-art method in the scenario where a battery is installed at the target home, and show that it outperforms the baseline by a clear margin.

The methods proposed in this thesis could benefit utility companies and end customers alike. For utility companies, higher solar disaggregation accuracy means that they can craft new rate programs, plan future investments to mitigate voltage problems, and manage bidirectional power flow

without installing separate meters at scale. Meanwhile, improving data efficiency translates to lowering the cost associated with solar disaggregation techniques, thereby increasing their application in the real world. For residential customers, solar disaggregation enables NILM, which in turn can help them understand how much money they spend on different appliances, especially energy-hungry appliances (e.g., air conditioner and furnace).

1.4 Outline of the thesis

Chapter 2 presents related works on NILM and solar disaggregation, followed by the description of the datasets that can be used for evaluating disaggregation methods. Then, we discuss the open challenges in the solar disaggregation area and put forward recommendations to address them in future work. Chapter 3 first describes the formulation of the solar disaggregation problem and lists the assumptions we make. Then, the models we use for estimating solar generation and home load are introduced. An iterative algorithm and an initialization technique are presented in our methodology framework. After that, in the experiment section, we first describe the dataset we use in the experiment, the different variations of our methods, and the baseline works used for performance comparison. Then we show the result in terms of disaggregation performance and the sensitivity of our method to the amount of net meter data used for disaggregation, the choice of solar proxies, and the weight initialization method. Lastly, we investigate whether a more accurate disaggregation technique could lead to higher accuracy in NILM.

Chapter 4 describes the extension of our previous work by considering BTM battery, presenting the whole disaggregation framework, the models we used for BTM components (i.e., solar generation, aggregated home demand, and battery activities) and the initialization techniques. Then, in the experiment section, we first describe the battery strategies we use in battery simulation and the baseline work. We also show the experimental results for solar disaggregation performance comparison, battery peak power estimation, and the sensitivity of our method to BTM battery operation strategy and battery

capacity. Chapter 5 concludes the thesis with some discussion about the limitations of the work presented in this thesis, threats to its validity and potential future extensions of this thesis.

Chapter 2

Related Work

2.1 Non-Intrusive Load Monitoring

Since the early days of smart meter rollouts, NILM has been extensively studied in the literature. At a high level, NILM methods aim to disaggregate the net load measured at a single point of measurement. A wide range of sampling rates are explored in the literature, from less than 1Hz to thousands of Hz. Despite the recent efforts in high-frequency range [49], [55], and the intuition that sampling the load profiles at high rates provides more useful features for NILM, collecting this data requires special hardware. The smart meter devices that are being installed widely in distribution grids can only provide low-resolution data. A recent study concludes that the data sampled at 1/30 Hz would be sufficient to achieve high accuracy in NILM [22]. It is also mentioned that such a low sampling rate allows the NILM algorithms to benefit from additional information pertaining to the past power consumption of some long-running appliances. A NILM method is proposed in [48] that is suitable for low-resolution data. The performance of this method is evaluated for a range of resolutions, from 5 minutes to 1 hour.

Since combining the temporal information with active power measurements can facilitate disaggregation [60], the most recent work utilizes Hidden Markov Model (HMM) and Deep Neural Networks (DNN). Reference [32] studies four variants of HMM for energy disaggregation using low-frequency data. Another low frequency power disaggregation method is proposed in [37] that is based on HMM and DNN. Reference [31] studies different deep learning architectures

for NILM. These methods can only generalize to unseen homes if the training set has enough variety, which is rare in NILM training sets. Reference [61] proposes a sequence-to-point learning via a Convolutional Neural Network (CNN) that outperforms the sequence-to-sequence method introduced in [31]. Reference [33] studies different DNN compression schemas and suggests a multi-task learning-based architecture to compress the models further.

The majority of NILM methods assume that the net load is simply the total power consumed by home appliances. There are just a few NILM papers that consider BTM solar generation. Reference [57] proposes a method to disaggregate three types of loads, namely traditional loads, distributed generation (e.g., PVs), and flexible loads (e.g., electric vehicles), at the substation level. However, the focus of our work is on customer-level load disaggregation. The closest line of work to ours is by Dinesh *et al.* [15], which proposes a NILM method for customers with BTM solar generation. The authors construct a unique set of signatures for appliances and solar generation, and classify their operating modes using a spectral clustering based method. Finally, they identify their state and operating mode through a subspace component power level matching algorithm. The main drawback of this approach is that it relies on the synthesized net load measured at 1 second intervals. This is much faster than the sampling rate of smart meters that are currently installed in many jurisdictions (which is typically in the order of minutes).

2.2 Solar Disaggregation

Several solar disaggregation techniques have been proposed to date drawing on algorithms from machine learning, signal processing, and state estimation. Table 2.1 summarizes these techniques. The vast literature on behind-the-meter solar disaggregation can be categorized into two classes based on the type of models they use for estimating solar power. In particular, in model-based techniques, PV systems are modelled using a physical PV model, while data-driven techniques develop a black-box PV model leveraging the training data.

Reference	Level	Rate	Category	Used Data	Approach
Ref. [3], [9]	Customer	1 hour	Model-Based	Lon. & Lat. of target home, Weather	Physical model, Machine Learning
Ref. [29], [30], [56]	Feeder	1 min	Data-Driven	NS, Reactive power at the feeder	Convex Optimization
Ref. [28], [54]	Customer	15 min	Data-Driven	NS, Ambient temperature	Convex Optimization
Ref. [13]	Customer	15 min	Data-Driven	NL, Local solar irradiance	Convex Optimization
Ref. [14]	Customer	1 hour	Data-Driven	NS, NL	Convex Optimization
Ref. [51]	Feeder	Multiple	Data-Driven	Local solar irradiance	Convex Optimization
Ref. [26], [27]	Customer	15 min	Model-Based	Weather, Local solar irradiance	Physical model, Optimization
Ref. [34]	Customer	1 hour	Data-Driven	NS, SC, Weather	Machine Learning
Ref. [45]	Feeder	30 min	Data-Driven	Ambient temperature, Local solar irradiance	State Estimation
Ref. [7]	Feeder	1 hour	Data-Driven	NS, NL	Optimization
Ref. [8]	Customer	1 hour	Data-Driven	NS, NL	Optimization
Ref. [36]	Feeder	1 hour	Data-Driven	NS	Machine Learning
Ref. [5]	Customer	30 min	Data-Driven	NS	Optimization

Table 2.1: Related work on disaggregation of behind-the-meter solar generation

2.2.1 Data-driven approaches

With the growing adoption of different metering technologies in distribution grids, data-driven methods have become increasingly popular.

Some of the methods rely on the aggregate data at the feeder, distribution, or substation transformer level. Kara *et al.* [29] developed a linear proxy-based estimator to disaggregate feeder-level solar generation from the aggregate real power at the substation, using reactive power data measured by a DPMU [39] and PV generation profiles from nearby metered PV systems. A similar method was proposed by Tabone *et al.* to tackle customer-level solar disaggregation [54] by utilizing the aggregated net load data at the substation level. But instead of using reactive power data to estimate the aggregate home load, they use temperature and time of the day. Both methods leverage a contextually supervised source separating [58] with different features. Bu *et al.* [7] utilize separately metered load and PV generation data of some customers to disaggregate higher-level net load using a game theoretic approach. They formulate solar disaggregation as a nested bi-layer optimization problem. This method adaptively updates the estimation in each time step and shows robustness to unobserved events and abnormalities (e.g., PV system failures). Shaffery *et al.* [45] propose a Bayesian Structure Time Series (BSTS) model for solar disaggregation. Unlike other data-driven methods, it can provide a probabilistic estimation of PV generation and load consumption, allowing the operator to determine necessary reserves. However, the slow training process limits its real-world application. The common shortcoming of these methods is that they are not accurate enough when applied to the net load of a single customer and sensors, such as distribution-level PMUs, are not yet available in large numbers in distribution grids. In another line of work, Sosan *et al.* [51] disaggregate the solar generation in the frequency domain given that the spectral density of the aggregated power flow is similar to the measured PV generation. The result of this method is promising enough to encourage researchers to use frequency domain analysis to address the disaggregation problem especially at the feeder-level where higher resolution data might be

available. In recent work [36], a model is trained via federated learning for community-level solar disaggregation while protecting user privacy.

Meanwhile, there are many methods that rely on customer-level net meter data. Cheung *et al.* [13] model demands of customers with PV systems using a mixture model of representative customers without PV systems which are selected via clustering. Leveraging the fact that customer-level net load curves have different shapes under different weather conditions, Li *et al.* [34] extract multiple features and feed them to machine learning models to infer PV capacity and estimate solar generation. In recent work [8], a disaggregation method is proposed based on the observation that there is a strong correlation between monthly nocturnal and diurnal homes loads. A shortcoming of this method is that it requires three years of historical data, which may not always be available for each customer. In [5] a novel approach is proposed to perform solar disaggregation in real-world situations where the amount of solar power exported to the grid is not reported by the smart meter.

To our knowledge, disaggregating solar power from net meter data in the presence of other BTM DER, like battery packs, has been studied in two recent papers only. Reference [14], which extends [13], utilizes proxy measurements from 15 solar sites to estimate solar generation. In contrast, our method needs as few as one real proxy thanks to additional synthetic proxies that are incorporated. We use it as our baseline for performance comparison in the experiments where customers have BTM batteries installed. The second paper [59] employs a contextually supervised source separation method with the addition of estimating the battery operation. The drawback of this method is that it assumes BTM batteries of different customers are controlled using the same strategy and utilizes this knowledge in the disaggregation process. In real world, the control strategy of batteries is not known a priori owing to the diversity of objective functions, pricing schemes, and power electronic interfaces.

2.2.2 Model-based approaches

Compared to data-driven approaches, model-based approaches normally require no or just a few data points for calibration. They learn the deployment characteristics of PV systems (e.g., capacity, tilt, orientation), which is useful for both real-time estimation and long-term forecasting. Reference [9] uses the PV system's location and net load data to build a model for maximum clear sky solar generation. It then estimates the true solar generation using a general weather model to account for the percentage reduction in the clear sky solar irradiance due to clouds, humidity, precipitation, etc. The method requires net load data from two days with clear sky and low energy consumption that have a large temperature difference. A solar disaggregation toolkit based on [9] is developed in [3], which is used as a baseline in our work.

Reference [26] proposes an unsupervised solar disaggregation framework that does not require net load data or the location of the PV system (i.e., its latitude and longitude). Instead, the authors estimate the home load by using a physical PV model together with Hidden Markov Model Regression. They start with an initial guess of the physical PV model parameters and iteratively estimate the home load and solar generation from the net load data. This method can achieve satisfactory performance after many iterations, which makes it too slow for real-world applications. In addition, accurate weather and irradiance data from the vicinity of the target home are necessary for accurate disaggregation. We use this method as a baseline. The authors extend this work in [27] to jointly disaggregate the net load data of a group of customers into aggregated solar generation and aggregated home load.

2.3 Open Data

Solar disaggregation studies use net metering data collected at different levels of aggregation. The customer-level data is available through AMI while the feeder-level data is typically collected by DPMUs or the SCADA system if there is such instrumentation beyond the distribution substation. For validation purposes, additional gross meters need to be installed behind the utility meter

to separately measure the solar inverter output.

The most popular dataset which has been used for evaluating solar disaggregation methods is released by *Pecan Street Inc.* [24]. It contains the customer-level measurement of solar generation and household demand for a total of 73 homes located in three states in the U.S. (New York, California, and Texas). Measurements cover three granularity levels, namely 1 second, 1 minute and 15 minutes. This is useful to evaluate a disaggregation algorithm at different temporal resolutions as we do in Section 2.4. We also use this dataset in Subsection 3.4.3 for quantifying the improvement in the accuracy of NILM techniques when they run on the disaggregated home load rather than the net load measured by a smart meter, since this dataset also contains the appliance-level consumption in each household. Another relatively large dataset is released by *Ausgrid*, a utility company in Sydney, Australia [2]. The half-hour household consumption and solar output data are collected from 300 customers with rooftop solar PV systems. The dataset spans 3 years, from July 1, 2010 to June 30, 2013, and contains the actual solar panel capacity for each customer. We use this dataset for measuring the disaggregation performance of our two proposed methods. Finally, the SunDance dataset [44] includes hourly net meter, solar generation, and weather data for 100 sites in North America.

To our knowledge, the above datasets are the only publicly available datasets that contain both solar generation and home load data. However, there are several residential load datasets which are published online [6], [23]. Real solar generation data from specific PV sites can be found in [44], [52]. Synthetic PV output can also be simulated using the System Advisor Model (SAM) developed by the National Renewable Energy Laboratory according to the real solar irradiation data and other weather data [40]. Therefore, a synthetic net metering dataset can be created easily by combining home load and solar generation from different sources.

2.4 Disaggregation Challenges

Despite several efforts to date to disaggregate solar power from net meter data there are several challenges which need to be addressed.

Low temporal resolution of customer-level data: Data collected by smart meters is coarse-grained (typically 1 sample every 15 minutes). This dramatically increases the difficulty of capturing inherent variability in solar generation and household demand, and prevents researchers from successfully separating frequency components of the two signals. High-frequency DPMU data can support the use of signal processing techniques. But since these sensors are typically installed at higher levels of aggregation in the distribution grid, fluctuations smooth out further due to aggregation.

To understand how the temporal resolution of input data could affect the performance of solar disaggregation algorithms when applied to data collected for individual customers, we run two model-based [3], [26] and two model-free [13], [54] approaches[1] proposed in the literature to disaggregate net meter data of five randomly selected homes in Austin, Texas. We run each algorithm three times for a given home, each time using the net meter data with a different resolution (1min, 15min, and 1hr). We obtain the net meter, home load, and PV generation data for a month in summer and a month in winter from the Pecan Street dataset and pull in 5-minute weather data (GHI, GNI, DNI, Temperature, etc.)[2] for the same periods for a location in Austin[3] (30.267°N,-97.743°E) from the Solcast API [50]. Note that a subset of these features are needed by each algorithm as specified in Table 2.1. We do not retune the (hyper)parameters of each algorithm across the three runs, and report normalized root-mean-square error (nRMSE) which is root-mean-square error normalized by the mean value of the measurements. For fair comparison, we only include the estimates at the top of the hour in the calculation of nRMSE as they are available for all three runs. As shown in Figure 2.1, increasing the

[1]We implemented [13] from scratch and [26] based on PV modelling code provided by the authors. We used the implementations of [3], [54] we found on authors' websites.

[2]For the 1min scenario, we use weather data of the closest 5 minute interval.

[3]The Pecan Street dataset does not include the home address, hence we queried weather data for a randomly selected location in downtown Austin.

temporal resolution does not improve the reliability of estimates in general. We believe this is because the algorithms are not designed to take advantage of high-resolution net meter data as it cannot be obtained from AMI today.

Abrupt and gradual changes in the output of PV systems: A number of different events can change the power output of a PV system over time. For example, inverter failure and panel cleaning will cause the PV output to change rapidly in a short period of time; while soiling on solar panels (i.e., the dry deposition of dust and light absorbing particles on the surface of the panel) will gradually decrease its power output. Traditional PV models cannot track these changes to adjust the estimated PV generation.

Latent flexibility: The continued rise in the adoption of BTM energy storage, demand-side management technologies, and smart thermostats in homes and buildings creates problems for most data-driven solar disaggregation models. This is because these components can change the load profile, but control policies used or price signals sent to them are not typically known when the disaggregation problem is solved. This latent flexibility is ignored in most previous work on solar disaggregation, except work [14] and work [59] which address the disaggregation problem in the presence of a BTM battery. [14] also shows that state-of-the-art approaches cannot accurately perform disaggregation when there is a BTM battery. Thus, future work should focus on developing disaggregation algorithms that can remove effects of latent components from net meter data through identification of control signals and actions.

Lack of datasets containing different types of households: Most datasets that can be used for evaluating solar disaggregation methods do not include information about households that participate in demand-response (DR) programs, installed smart thermostats or BTM solar-plus-storage systems in the metadata. Specifically, from the three datasets described in Section 2.3, only the Ausgrid dataset records whether the customer participated in a DR program. Even when this information is available, it is unclear what control or price signals were sent to those households.

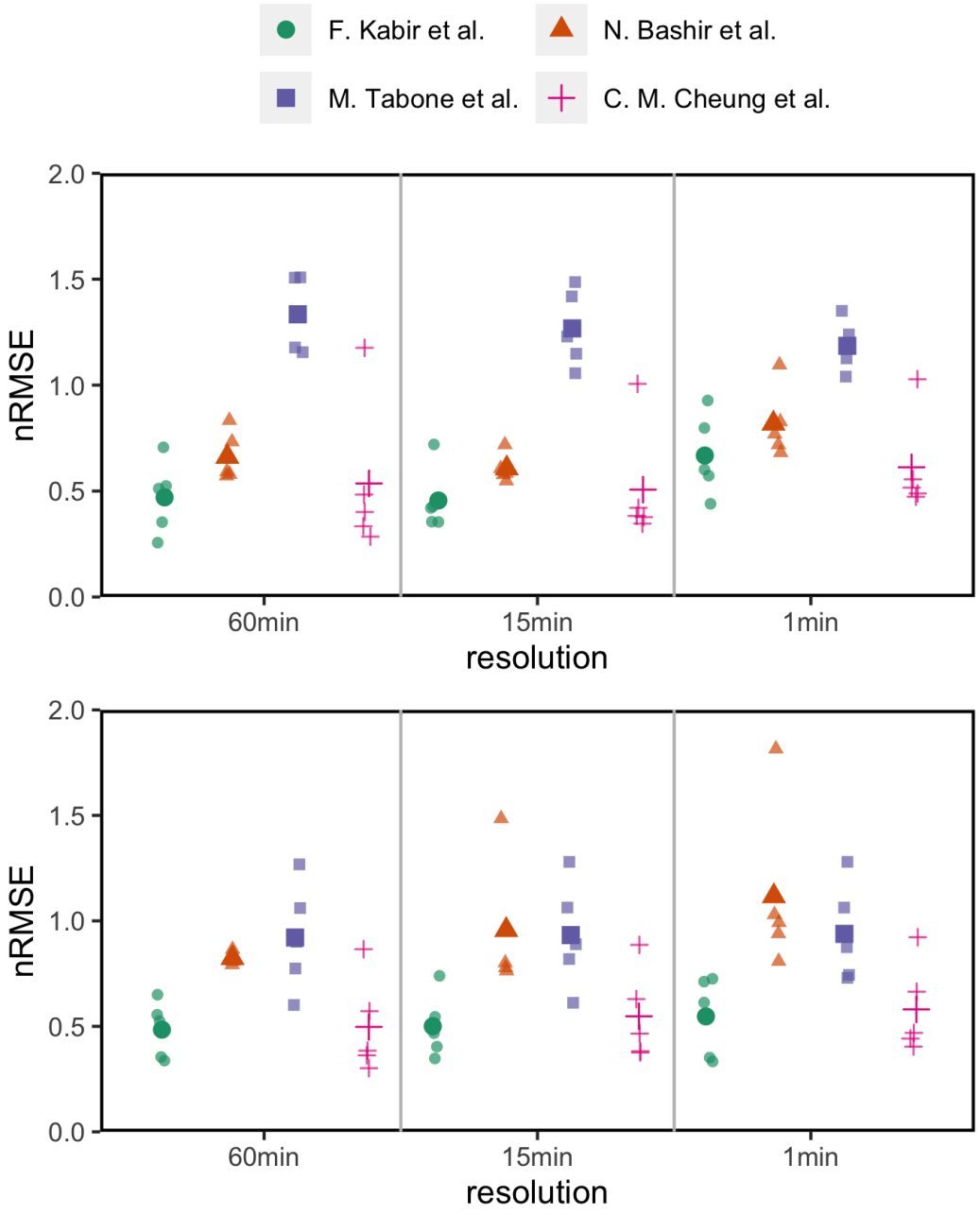

Figure 2.1: nRMSE of 4 disaggregation methods at different temporal resolutions. Each small marker shows the result of a single home. Each large marker indicates the nRMSE of one method averaged over 5 homes. The top figure shows performance results from 2018/06/01 to 2018/06/30 and the bottom one shows performance results from 2018/12/03 to 2018/12/30.

2.5 Research Opportunities

Several interesting research questions are still to be addressed, some of which will require overcoming the challenges described in the previous section. We outline these opportunities below.

Fusion of customer-level and feeder-level data: In recent years high frequency (up to hundreds of Hz) measurements of real and reactive power have become available thanks to the deployment of DPMUs in the secondary side of the substation. Fusing this data with smart meter data and incorporating pseudo-measurements in the disaggregation method is an interesting direction that can improve the overall accuracy and allow for running the disaggregation method in an online fashion.

Dynamic disaggregation algorithms: As noted in the previous section, the power output of a PV system can change over time due to various reasons. Thus, the PV models trained/calibrated using historical data can no longer provide accurate estimates of solar generation. Dynamic disaggregation enables researchers to simultaneously solve system identification and solar disaggregation problems, presumably at two different timescales. This way the changes in the power output of a PV system can be detected and the PV models can be updated accordingly.

Single-channel blind source separation (BSS) which separates a set of source signals from a single mixed signal is a perfect fit for the solar disaggregation problem. Hence, different techniques used in BSS can be modified and applied to this problem.

Utilizing various data sources: As the Internet of Things (IoT) devices are becoming ubiquitous across the building sector, there is a huge potential to use the data collected by their embedded sensors to better predict the home load. For example, the occupant presence and actions have an impact on the household demand. Hence, utilizing the occupancy data which is recorded by smart thermostats or plug load energy use collected by submetering devices can improve the accuracy of several data-driven disaggregation techniques.

Increasing data efficiency: Since historical (disaggregated) data regarding

solar generation and home load is usually unavailable from a customer with BTM PV system, the disaggregation problem must be solved in an unsupervised or semi-supervised fashion. Nevertheless, many methods proposed in related work [7], [8], [14], [54] assume the availability of measurements from a large number of neighboring PV systems, located in the same city or district as the customer's, to estimate solar power produced by BTM systems. This assumption does not typically hold in practice. Hence, it is essential to design a solar disaggregation method that requires measurements from no more than a few neighboring PV systems.

Building a framework for evaluating solar disaggregation algorithms: The lack of publicly available datasets that contain mixed and unmixed signals, open-source implementation of benchmark algorithms, and consensus on the evaluation metrics[4] has made it difficult to compare the methods proposed for solar disaggregation. We believe a comprehensive evaluation toolkit, similar to NILMTK [4], can greatly facilitate research in this area. Alternatively, benchmark solar disaggregation algorithms can be added to existing NILM evaluation frameworks; this would make sense since solar generation must be separated from net meter data before running NILM algorithms.

In the following chapters of this thesis, we first investigate one of the opportunities listed above, namely increasing data efficiency of solar disaggregation methods. We try to address some of the challenges related to latent flexibility by incorporating BTM battery in our disaggregation method.

[4]The following metrics have been used in related work to report the accuracy of a solar disaggregation algorithm: RMSE, MAPE, and coefficient of variation of RMSE.

Chapter 3

Solar Disaggregation without Battery

In this chapter, we propose a data-efficient solar disaggregation method for customers with PV installations only. Section 3.1 presents the solar disaggregation problem formulation and states the assumptions we make. Section 3.2 introduces the disaggregation algorithm as well as the models that are used in this algorithm. Then Section 3.3 describes the dataset and different variations of our methods. Furthermore, it introduces two baselines that we use for comparison. Finally, Section 3.4 shows the results in terms of disaggregation performance and discusses the sensitivity of our model to the amount of net meter data used for disaggregation, the choice of solar proxies, and the weight initialization method. In that section, we also investigate whether a more accurate solar disaggregation technique could lead to higher accuracy in NILM.

3.1 Problem Definition

Customer-level solar disaggregation concerns decomposing the customer's net load, presumably measured by a smart meter, into home load and solar generation. Since historical (disaggregated) data regarding solar generation and home load may not be available from a customer with a BTM PV system, the problem should be solved in an unsupervised or semi-supervised fashion.

3.1.1 Notation

As a general rule, matrices and vectors are denoted respectively by bold face uppercase and lowercase letters. We use a subscript to refer to a specific row of a matrix or an element of a vector.

Let $\mathbf{y} \in \mathbb{R}^T$ be a vector that collects the measured net load of one customer over T intervals. Hence, $\mathbf{y}_t$ denotes the net load measurement of this customer at time $t \in \{1, 2, ...T\}$. Similarly, let $\hat{\boldsymbol{\ell}}, \hat{\mathbf{s}} \in \mathbb{R}^T$ denote respectively their estimated home load and behind-the-meter solar generation in the same period. These quantities must satisfy the following equality constraint: $\mathbf{y} = \hat{\boldsymbol{\ell}} - \hat{\mathbf{s}}$.

Let $\mathbf{X}^A \in \mathbb{R}^{T \times K_a}$ be the set of K_a features that determine the customer's home load, and $\mathbf{X}^S \in \mathbb{R}^{T \times K_s}$ be the set of K_s proxy measurements that can be used to approximate the customer's solar generation via a mixture model. We can train a non-linear model g to map the features to the home load, and a linear solar mixture model to estimate the customer's solar generation. The model g can be a neural network, a support vector machine, a random forest, or any other nonlinear model used for regression. We can write:

$$\hat{\boldsymbol{\ell}} = g(\mathbf{X}^A; \boldsymbol{\theta}), \tag{3.1}$$

$$\hat{\mathbf{s}} = \mathbf{X}^S \mathbf{w}, \tag{3.2}$$

where $\boldsymbol{\theta}$ is a vector that represents parameters of the load model, and $\mathbf{w} \in \mathbb{R}^{K_s}$ is the weight vector of the mixture model. Hence, $\mathbf{w}_k$ is a scalar that represents the weight assigned to the k^{th} proxy. The motivation for using a linear mixture model for estimating solar generation is explained in Section 3.2.

3.1.2 Assumptions

We postulate that no information is available about the customers except their approximate location (i.e., the city or district they are located in) and their smart meter data. Hence, we do not know the exact longitude and latitude information of each customer. This is a reasonable assumption because (a) some customers are reluctant to provide their home address, and (b) there might be data privacy requirements that prevent the utility from sharing their

address with a third party that performs solar disaggregation or NILM. In addition to the smart meter data, solar irradiance, wind speed, and ambient temperature at the city scale can be downloaded via an API. We assume that deployment characteristics of BTM PV systems are not known a priori. These include the panel size, orientation, tilt, temperature coefficient, etc.

We assume that there is at least one separately metered solar installation in the same city or district as our target home. This site provides proxy measurements that are used to estimate solar generation of the target home. The deployment characteristics of this site could differ from the characteristics of the PV system installed at the target home. We argue that this is not a strong assumption as utilities usually have access to direct solar measurements from several sites in a city. Moreover, the cost of installing and maintaining one or a few PV systems can be easily justified by the potential benefits of observing customer-level PV generation.

3.2 Methodology

We now introduce the models we use for estimating solar generation and home load. We present our solar disaggregation algorithm, which has two main parts: a weight initialization technique and an iterative algorithm for updating the model parameters. Figure 3.1 shows the overview of our proposed solar disaggregation method.

3.2.1 Models

Solar mixture model: We aim to approximate that solar power generated by the BTM PV system installed at the target home using a mixture of proxy measurements from PV systems located in the same city or district. The intuition behind this approximation is that PV systems in the same geographical area have more or less the same solar generation pattern regardless of their deployment characteristics. This can be verified by inspection of Figure 3.2 which displays the solar power generated by 20 homes with BTM PV systems in Sydney, Australia. The PV systems that have the same orientation but

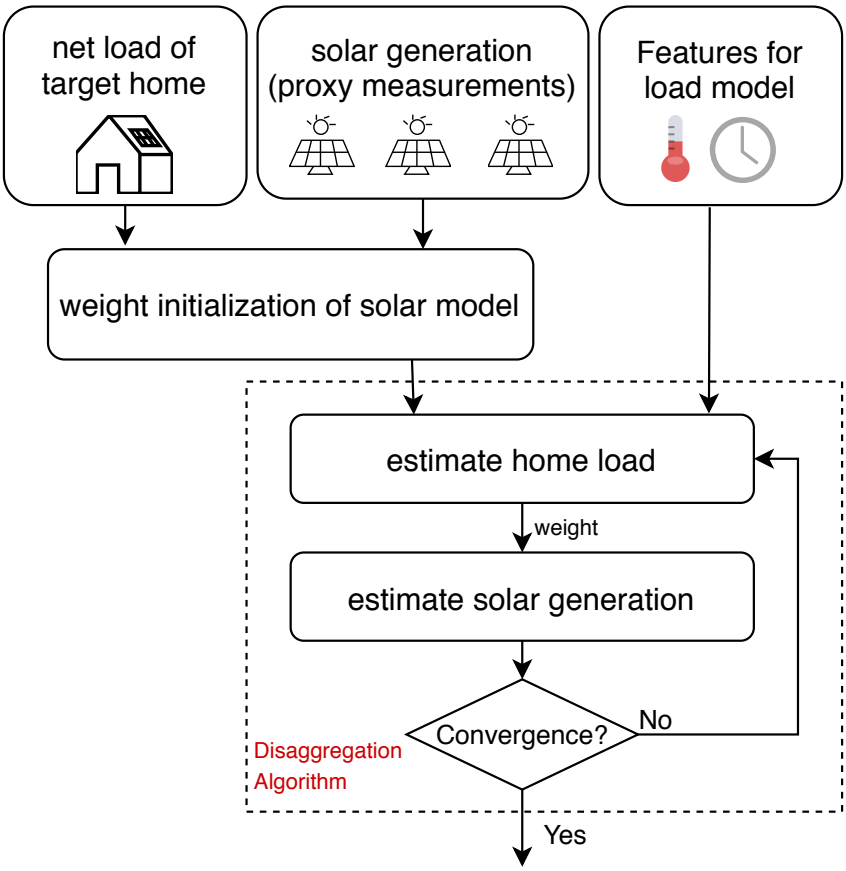

Figure 3.1: Overview of the proposed solar disaggregation method.

different sizes and tilts have almost identical solar generation patterns, though with different scales.

There are two specific challenges that must be addressed to get a good approximation. First, we do not have control over the deployment characteristics of the PV systems that provide proxy measurements. If they had exactly the same orientation angle as the PV system installed at the target home, estimating the target home's solar generation would reduce to learning a single scaling factor. One way to address this challenge is to adopt a solar mixture model to approximate the target home's solar generation as a weighted sum of a number of proxy measurements, as shown in Equation (3.2). This increases the chance of getting proxy measurements from PV systems with similar deployment characteristics to the target home. A higher weight will be eventually assigned to these PV systems in the mixture model. The second

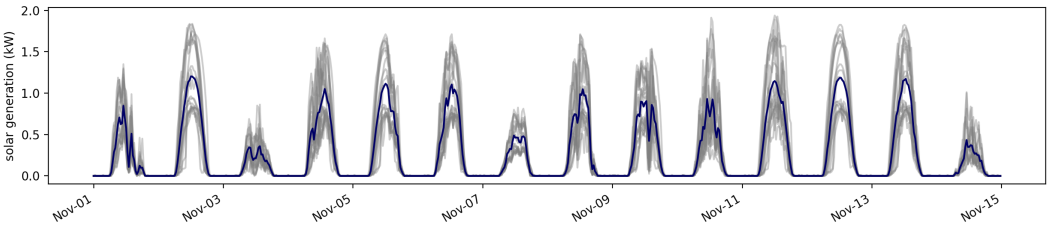

Figure 3.2: The solar generation of 20 homes in the Ausgrid dataset over 2 weeks. The thicker line shows the average solar generation power across all the homes.

challenge is that proxy measurements from a large number of neighbouring PV systems might not be available in practice. To address this challenge, we combine proxy measurements from real PV systems with measurements synthesized by a physical PV model that takes into account solar irradiance data of an arbitrary location in the same city. We discuss in Section 3.4 that it is essential to use proxy measurements from at least one real PV system as some fluctuations in solar generation cannot be accurately explained by the physical PV model when coarse-grained solar irradiance data is fed to this model. We also demonstrate the importance of incorporating synthetic proxies that have different orientation angles in Figure 3.7. These synthetic proxies help us estimate the peak time of solar generation more accurately.

The physical PV model that we use to obtain data for *synthetic proxies* is based on PVWatts [17]. Figure 3.3 shows a screenshot of the PVWatts calculator. We develop this model using the PV Performance Modeling Collaborative [53]. The output power of the PV model with the specified rating P_{dc0} can be computed given the transmitted plane of array (POA) irradiance I_{tr} and cell temperature T_{cell}:

$$P_{dc} = \frac{I_{tr}}{E_{ref}} P_{dc0}(1 + \gamma(T_{cell} - T_{ref})) \tag{3.3}$$

Here γ represents the temperature coefficient, E_{ref} represents the reference irradiance, and T_{ref} represents the reference cell temperature. We set them respectively to -0.47%/$^{\circ}C$, 1000W/m^2, and 25$^{\circ}C$ to create synthetic proxies. I_{tr} is determined by solar irradiance data (direct normal irradiance, diffuse horizontal irradiance, global horizontal irradiance), PV system characteristics

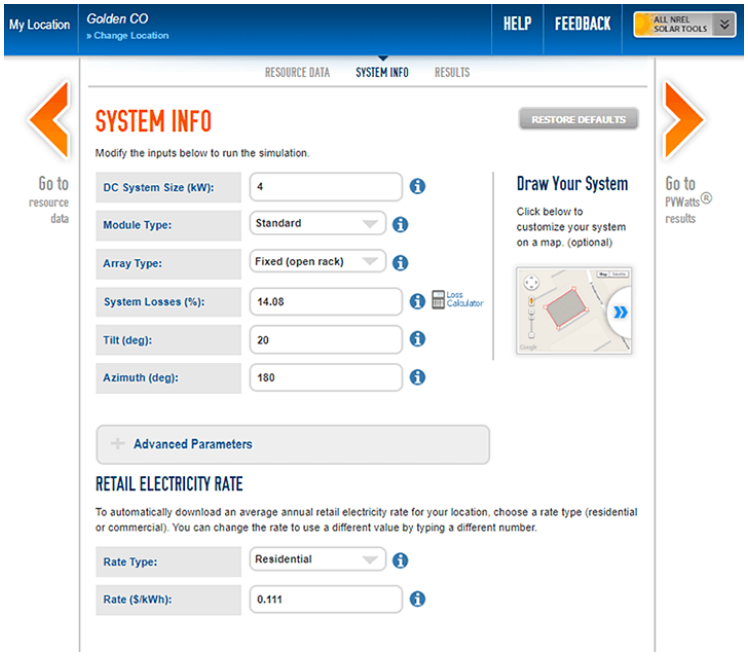

Figure 3.3: Screenshot of PVWatts calculator developed by National Renewable Energy Laboratory (NREL).

(e.g., tilt, orientation) and its location. T_{cell} is a function of wind speed, ambient air temperature, and solar irradiance data. We use different preset technical parameters for different synthetic proxies.

Home load model: To estimate the home load, we adopt random forest regression, a supervised learning algorithm that uses an ensemble learning method for regression. We use the scikit-learn [43] library to train this model. Four explanatory variables are used as features, $\mathbf{X}^A$, for all customers. These variables include ambient temperature $\mathbf{c}$, exponentially weighted moving average of temperature over the last 24 hours $\mathbf{c}_{wmv}$, hour of the day $\mathbf{h}$, and a binary variable $\mathbf{d}$ that indicates if it is a weekday or weekend. Thus, we have $\mathbf{X}^A = [\mathbf{c}, \mathbf{c}_{wmv}, \mathbf{h}, \mathbf{d}]$.

3.2.2 Solar Disaggregation

Solar model weight initialization: $\text{InitSolar}(\mathbf{y}, \mathbf{X}^S)$

The first step of our method is to initialize the weight vector $\mathbf{w}$ of the solar mixture model using the net load data of the target home and the solar generation data collected from the proxies. A good initialization can enhance the

performance of the disaggregation method and reduce its convergence time. Our weight initialization method has 3 main steps:

1. Estimating the physical characteristics of PV systems installed at the target home and real solar proxies.

2. Finding the maximum solar generation of each PV system.

3. Solving an optimization problem to determine the initial weight vector $\mathbf{w}^0$.

We use an open source toolkit, SolarTK [3], to estimate the physical characteristics of PV systems including its tilt, orientation, and panel size. To estimate these parameters, the toolkit takes the real solar generation data as input and finds the maximum solar generation. We can run this toolkit on proxy measurements, but we lack the real solar generation data from the target home. To solve this problem, we approximate the solar generation of the target home given the net load data $\mathbf{y}$ from this expression $\hat{\mathbf{s}} \approx [\ell_{base} - \mathbf{y}]^+$, where $[\ \ ]^+$ is an operator that truncates negative elements of a vector to zero, and ℓ_{base} is the target home's base power consumption calculated as the minimum consumption level at night time. SolarTK is then applied to the estimated solar generation of the target home and the real solar generation of solar proxy/proxies to obtain the estimated parameters for all PV systems. Since we use a city's longitude and latitude as an approximate location for all the PV systems located in it, the estimated parameters may not be highly accurate.

We then calculate the maximum solar generation for each proxy and target home using the estimated deployment characteristics obtained in Step 1. The maximum solar generation is the potential generation of a PV system under clear sky condition, that is determined by the system's physical characteristics, the ambient temperature and the location of PV. We denote the maximum solar generation of the k^{th} proxy by $\mathbf{m}_k^p \in \mathbb{R}^T$, and the maximum solar generation of target home by $\mathbf{m}^c \in \mathbb{R}^T$.

In the last step, we determine the initial weight vector, $\mathbf{w}$, for the solar mixture model following the idea of [47], [51]; the solar generation of a target home with unknown deployment characteristics is estimated utilizing metered solar generation of sites with nonuniform deployment characteristics. Formally, we can write

$$\mathbf{s}_t^{target} = \alpha \cdot \mathbf{s}_t^{proxy} \tag{3.4}$$

where α depends on time, site location, and other site-specific factors. In our method, we simplify α to be a constant weight factor for each site, i.e., $\mathbf{w}_k$. Since we do not have the true solar generation from target home in Equation (3.4), we use the maximum solar generations to determine the initial weight of each solar proxy. Specifically, the weight factor $\mathbf{w}_k$ for the k^{th} proxy can be determined by solving the following optimization problem:

$$\begin{aligned} \min_{\mathbf{w}_k} \quad & \|\mathbf{w}_k \cdot \mathbf{m}_k^p - \mathbf{m}^c\|_2 \\ \text{subject to} \quad & \mathbf{w}_k > 0 \end{aligned} \tag{3.5}$$

Finally, the initial weight vector is $\mathbf{w}^0 = \mathbf{w}/K$ and initial solar estimation is $\mathbf{s}^0 = \mathbf{X}^S \mathbf{w}^0$. Here K is the number of solar proxies.

Disaggregation algorithm: In this step, we iteratively estimate the home load and solar generation until the parameters of our model converge. Algorithm 1 presents the pseudocode of the proposed solar disaggregation algorithm. After obtaining the initial weights $\mathbf{w}$ for the solar mixture model, we first estimate the solar PV generation $\mathbf{s}^{iter}$ using a linear combination of the solar proxies. Then, we use $\mathbf{y} = \hat{\boldsymbol{\ell}} - \hat{\mathbf{s}}$ to calculate the estimated home load $\boldsymbol{\ell}^{iter}$ (line 2) and incrementally train the load model using $\boldsymbol{\ell}^{iter}$ and load related features $\mathbf{X}^A$ (line 3). Based on the updated home load $\boldsymbol{\ell}^{iter}$ (line 4), we determine solar generation $\mathbf{s}^{iter}$ (line 5), update the weights for solar proxies (line 6), and recalculate the solar generation using the updated weights (line 7). We repeat the above steps until the solar proxy weights $\mathbf{w}$ converge or we reach the maximum number of iterations. In our experiments, it typically takes between 20 and 80 iterations for this algorithm to converge depending on the number of proxies and goodness of initial weights.

Algorithm 1: SolarDisaggregationWithoutBattery($\mathbf{y}, \mathbf{X}^S, \mathbf{X}^A$)

Input : Net load of the target customer, $\mathbf{y} \in \mathbb{R}^T$;
Proxy measurements from K sites, $\mathbf{X}^S \in \mathbb{R}^{T \times K_s}$;
Load related ambient features, $\mathbf{X}^A \in \mathbb{R}^{T \times K_a}$;

Output: Estimated solar generation and home load of the target customer, $\hat{\mathbf{s}}$, $\hat{\boldsymbol{\ell}}$;

Init: $\mathbf{s}^0, \mathbf{w}^0 \leftarrow InitSolar(\mathbf{y}, \mathbf{X}^S)$;
Initialize parameters $\boldsymbol{\theta}^0$ for load model g;

while $iter < Max\ Iteration$ ***and*** $|\boldsymbol{w}^{iter} - \boldsymbol{w}^{iter-1}| > \epsilon$ **do**
  $\boldsymbol{\ell}^{iter} \leftarrow \mathbf{s}^{iter} + \mathbf{y}$;
  Incrementally train the model g with input feature $\mathbf{X}^A$ and output $\boldsymbol{\ell}^{iter}$;
  Update load $\boldsymbol{\ell}^{iter} \leftarrow g(\mathbf{X}^A, \boldsymbol{\theta}^{iter})$;
  $\mathbf{s}^{iter} = \boldsymbol{\ell}^{iter} - \mathbf{y}$;
  $\mathbf{w}^{iter} \leftarrow \text{argmin}_{\mathbf{w}} \|\mathbf{X}^S\mathbf{w} - \mathbf{s}^{iter}\|_2$;
  $\mathbf{s}^{iter} \leftarrow \mathbf{X}^S\mathbf{w}^{iter}$;
end

3.3 Evaluation

3.3.1 Dataset

We use the Ausgrid [2] dataset to evaluate the estimation accuracy of different solar disaggregation methods. This dataset includes 30-minute resolution net load measurements in addition to direct measurements of home load and solar generation from homes with rooftop PV systems. It consists of 140 customers with rooftop PV systems in Sydney, Australia (in the southern hemisphere) with the latitude and longitude of -33.888575 and 151.187349 respectively. Figure 3.4 shows the locations of these customers[1]. These locations are approximate since we only have the postal code of each customer. It is also likely that a marker in this figure represents multiple customers that have the same postal code. Since Sydney is a sprawling city, we cluster the customers into three clusters according to their latitude and longitude. Points within each cluster are drawn in the same color and shape in Figure 3.4. As it can be seen, each cluster still spans a large area of the city. We consider two periods in two seasons, one from November 1, 2012 to November 30, 2012 in the sum-

[1]The map is downloaded from OpenStreetMap [42].

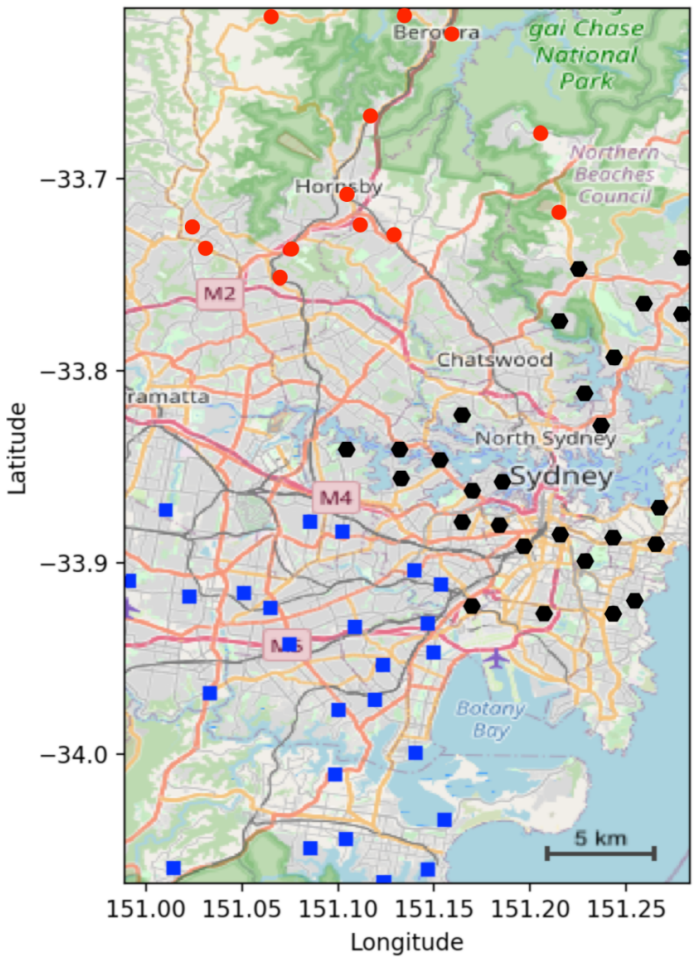

Figure 3.4: The approximate locations of customers in Ausgrid dataset. The unit of scale bar is 5 km.

mer season (T=1440) and the other one from May 1, 2013 to May 30, 2013 in the winter season (T=1440). A small number of customers are removed due to data quality issues in each season. For Sydney's weather data, we pull the solar radiation, wind speed, and outside air temperature with 30-minute temporal resolution using the Solcast API [50].

3.3.2 Variants of our Disaggregation Method

We implement our method with 4 different solar proxy settings.

- **3Proxies:** we directly use solar generation data for the same periods from 3 real rooftop PV systems in the same city.
- **1P+1SP:** we only use 1 real solar proxy combined with 1 synthetic

Table 3.1: Physical parameters of synthetic proxies we set in different proxy settings.

Method	orientation (°)	tilt (°)	DC rating (kW)
1P+1SP(SP1)	0	33.9	3
1P+3SP(SP1)	0	33.9	3
1P+3SP(SP2)	90	33.9	3
1P+3SP(SP3)	270	33.9	3

1P+3SP(SPx) refers to the x^{th} synthetic proxy in 1P+3SP; The panel faces respectively N, E, S, and W when the orientation angle is 0°, 90°, 180°, 270°.

proxy. In this case, the ideal orientation angle in each hemisphere is used to create the synthetic proxy. It is specifically 180° in the northern hemisphere and 0° in the southern hemisphere.

- **1P+3SP:** we use 1 real solar proxy combined with 3 synthetic proxies with different orientation angles.
- **3SP:** we use 3 synthetic proxies with different orientation angles just like the previous setting.

The parameters for different synthetic proxies are shown in Table 3.1. We set the tilt angle to the absolute value of the city's latitude and use a uniform DC rating for all synthetic proxies. The tilt and DC rating have a similar effect on solar generation curve, i.e., they scale the curve up or down [9], whereas the orientation shifts the peak of the generation curve to earlier or later. Therefore, we can set the tilt angle and DC rating similarly for all the synthetic solar proxies because the elements of our weight vector $\mathbf{w}$ will be adjusted by Algorithm 1.

3.3.3 Baselines

We compare the performance of our solar disaggregation method with two methods that also use the data that is commonly available to the utility and outperform other solar disaggregation methods proposed in the literature. Specifically, we use the solar disaggregation methods proposed in [26] and [3] as our baselines; these methods are labelled "Baseline 1" and "Baseline 2",

respectively. For a fair comparison, we implement the one-nearby-proxy-based solar estimation method in [3] that was adopted in the case study of computing the clear sky index. In each experiment, we use the same real solar proxy for our method and Baseline 2. It is worth mentioning that in some homes the PV system's physical characteristics estimated by Baseline 2 can be quite different from their true values due to the inaccuracy of location information and lack of directly measured solar generation from the respective homes. Therefore, in our implementation of Baseline 2 we constrain the system's orientation within specific bounds based on the hemisphere in which the home is located.

3.3.4 Evaluation Metrics

We use two metrics to assess the performance of our disaggregation method with different proxies, and compare them with the two baselines. The first metric is the root-mean-square error (RMSE) which has been used in many solar disaggregation papers. The second one is a normalized RMSE metric, called nRMSE. It is the RMSE normalized by the mean value of the real solar generation.

$$nRMSE = \frac{\sqrt{\sum_{t=1}^{T}(\mathbf{s}_t - \hat{\mathbf{s}}_t)^2/T}}{\sum_{t=1}^{T}\mathbf{s}_t/T} = \frac{\text{RMSE}}{\text{Mean}} \tag{3.6}$$

Compared to RMSE, this normalized metric can help us compare the disaggregation performance on signals with different magnitudes (i.e., generation from PV panels with different sizes). These two are the performance metrics used in related work that focuses on solar disaggregation[2].

3.4 Experimental Results

We first evaluate the performance of our methods in disaggregating BTM solar generation using the metrics introduced in the previous section. We analyze the sensitivity of our methods to the amount of net meter data used for disaggregation, the choice of solar proxies, and the weight initialization method.

[2]The mean absolute percentage error (MAPE) is occasionally used besides RMSE and nRMSE as a performance metric for energy disaggregation. But MAPE is not well defined in this case because the true output of the PV system can be zero in some intervals.

Table 3.2: Comparison of disaggregation methods for the customers without BTM battery systems. Each cell contains two slash-separated metrics: average RMSE and nRMSE over all customers.

	Summer		Winter	
Method	Solar	Load	Solar	Load
3Proxies	0.0590/0.450	0.0590/0.229	0.0576/0.761	0.0576/0.201
1P+1SP	0.0683/0.517	0.0683/0.270	0.0646/0.829	0.0646/0.228
1P+3SP	**0.0649/0.498**	**0.0649/0.252**	**0.0618/0.791**	**0.0618/0.216**
3SP	0.0780/0.596	0.0780/0.305	0.0664/0.826	0.0664/0.233
Baseline 1	0.0765/0.606	0.0765/0.283	0.1168/1.696	0.1168/0.375
Baseline 2	0.0853/0.632	0.0853/0.338	0.0772/0.947	0.0772/0.280

Lastly, we investigate the impact of running NILM methods on the disaggregated solar generation, real solar generation, and net load. This will reveal the potential benefits of disaggregating solar generation prior to performing NILM.

3.4.1 Disaggregation Performance

We compare 4 variants of our method – 3Proxies, 1P+1SP, 1P+3SP, and 3SP – with the two baselines described in Section 3.3.2. For each variant, we evaluate the disaggregation performance for all customers with PV systems in the dataset. Since our method utilizes proxy measurements, we run the experiment 10 times for each target home with real solar proxies that are randomly selected from the same cluster as the target home, excluding that home (shown in Figure 3.4).

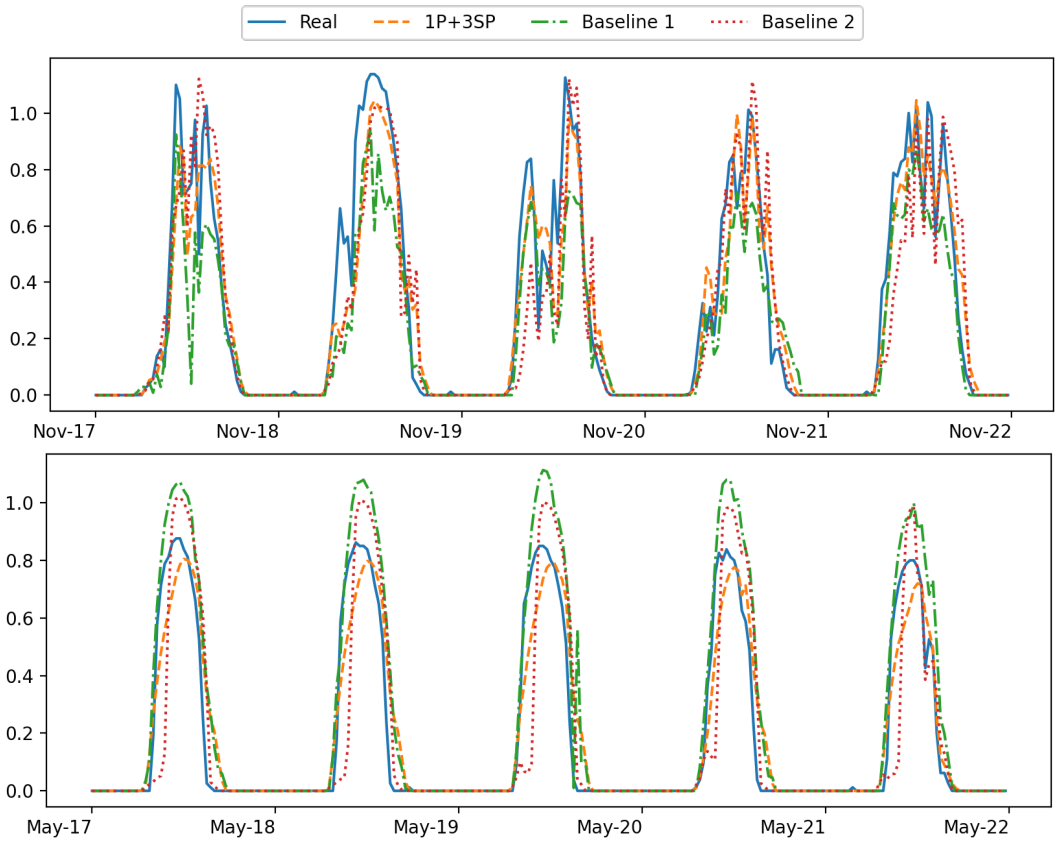

Figure 3.5: Comparison of disaggregated 30-min average solar generation power (in kW) in summer (top) and winter (bottom) for a customer without BTM battery storage over five days.

Estimation accuracy: Table 3.2 shows the average RMSE and nRMSE of solar generation and home load estimation across all customers in two seasons. We observe that using 3 real proxies (3Proxies) yields the lowest error compared to the other variants of our method and the two baselines. That aside, 1P+1SP outperforms the two baselines in both seasons, reducing the RMSE of solar estimation by 28.20% and 18.07% on average, respectively. Similarly, 1P+3SP outperforms the two baselines in all cases, reducing the RMSE of solar estimation by 31.59% and 21.87% on average compared to Baseline 1 and Baseline 2, respectively. This observation suggests that by utilizing real data from as few as one directly measured PV site, we can disaggregate solar power and home load more accurately than the state-of-the-art solar disaggregation methods. Comparing the result of 3Proxies with 1P+3SP, we see a trade-off between the disaggregation accuracy and the cost of acquiring data

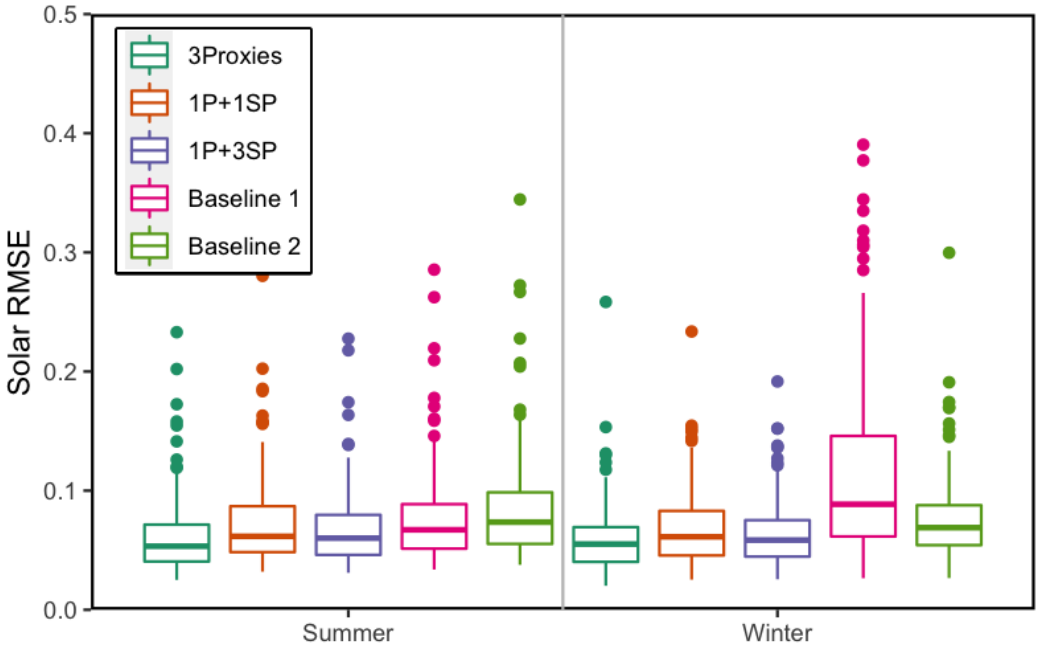

Figure 3.6: The RMSE distribution for homes in the Ausgrid dataset in two seasons (without considering batteries). The legend shows the solar disaggregation methods shown in each panel (from left to right). The whiskers show $1.5 \times$ IQR.

from real proxies. The end users can choose the best proxy setting for different tasks (e.g., NILM, and solar modelling and forecast) according to their budget, access to data, and required accuracy level. Furthermore, using 3 synthetic proxies with distinct orientation angles proves to be better than using only the best orientation angle for the southern hemisphere as PV installations in Sydney do not necessarily have the same (ideal) orientation angle. Interestingly, 3SP has the worst performance among the four variants of our method, although it still beats Baseline 1 and Baseline 2 in winter. This underscores the importance of having at least one real proxy for solar disaggregation to account for high-frequency variations in solar generation (e.g., due to passing clouds). We do not consider 3SP in the following sensitivity analysis experiment as it does not use a real proxy. Figure 3.5 illustrates solar generation disaggregated by our method with 1P+3SP and the two baseline methods for a randomly selected home in summer and winter. It can be seen that our estimate of the PV output is generally closer to the true output considering

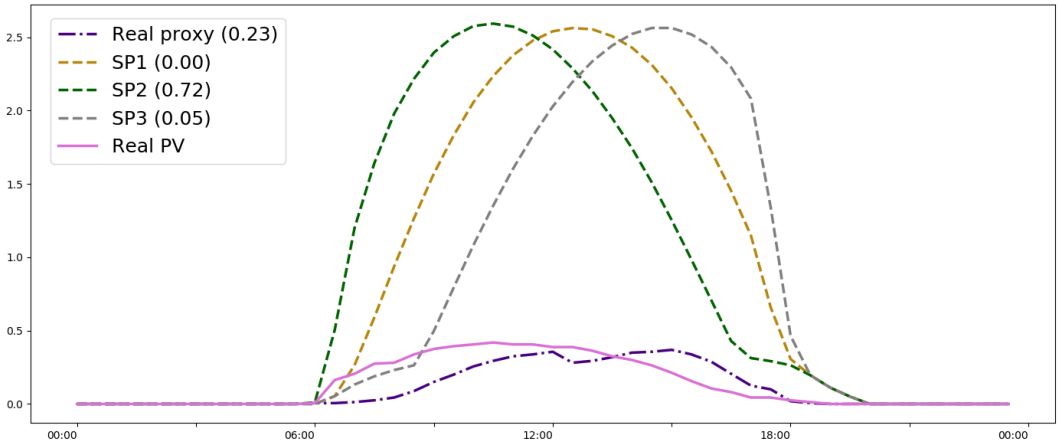

Figure 3.7: PV generation (kW) of a sample home. Dashed curves show solar proxy measurements. The relative weights (normalized to sum to 1) of proxies are put in the legend.

both the peak generation time and scale. Figure 3.6 is the box and whisker plot indicating the RMSE distribution of all customers for each disaggregation method. It can be seen that all methods have a large variance in both seasons, and in winter there are several customers with RMSE values outside the 1.5 times the interquartile range. In spite of this, the 1P+3SP variant of our method outperforms both baselines and the 1P+1SP variant for almost all homes. In a few homes, the performance of the 1P+3SP variant is on par with Baseline 2, which utilizes proxy measurements from one neighbouring PV site. This suggests that using synthetic proxies in addition to one real proxy improves the estimation accuracy in most cases.

Figure 3.7 shows real solar generations of a target home besides the four proxy measurements used in 1P+3SP. It can be seen that the peak generation of the target home and real solar proxy happen at different times as they have different orientations. In this case, the synthetic proxy with an orientation angle close to the target home's orientation angle gets a much higher weight compared to the other synthetic proxies and the real proxy. This highlights the advantage of incorporating the synthetic proxies.

Computation time: We now compare our method (the 1P+3SP variant) with the baselines in terms of their running time. Excessively high running times could be prohibitively costly for the utilities that intend to run the solar

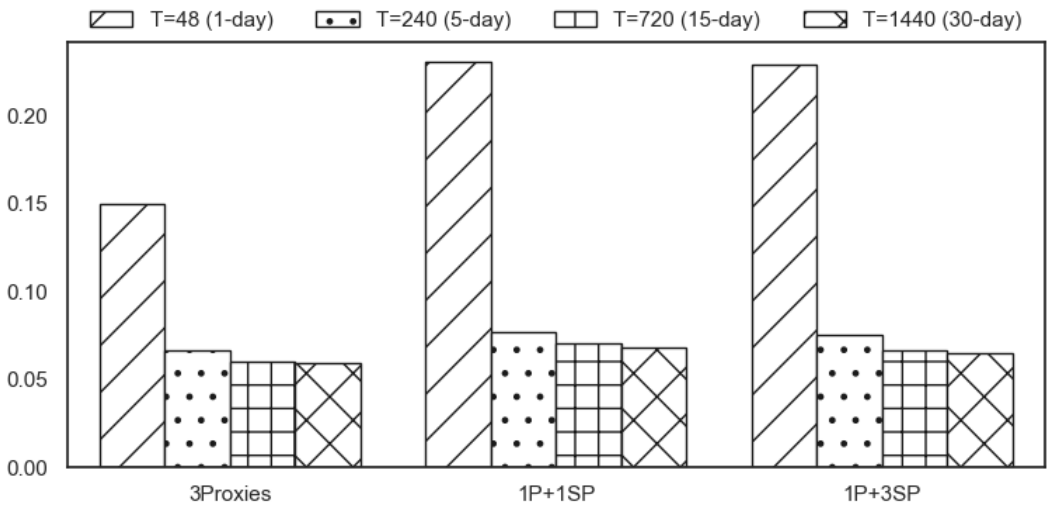

Figure 3.8: Average RMSE of disaggregated solar for different disaggregation lengths in the Ausgrid dataset.

disaggregation method at scale. We use an Intel Xeon Silver 4114 CPU to run the experiments. The total running time for disaggregating one month data from a target home in Ausgrid using 1P+3SP is around 35 seconds (25 seconds for weight initialization and 10 seconds for solar disaggregation). The other variants of our method have similar running times. In comparison, the total running time of Baseline 1 is about 70 minutes, which is roughly 120 times greater than the running time of our method. We attribute this to the fact that this method solves a nonlinear optimization problem for the solar model and trains a Markov switching regression model for load estimation in every iteration. Although Baseline 2 has a running time that is similar to our proposed method (i.e., 30 seconds), its estimation accuracy is worse than ours as explained in the previous section.

3.4.2 Sensitivity Analysis

Disaggregation length: We now investigate how extending the length of solar generation data would impact the performance of our disaggregation method. We set the disaggregation length T to be {48, 240, 720, 1,440} time intervals corresponding to {1, 5, 15, 30} days of data from Ausgrid. Then, we apply our method to each T consecutive intervals separately. Similar to

the implementation in the previous subsection, we run 10 independent experiments and average the error values for each target home to account for the randomness caused by choosing different solar proxies. Figure 3.8 shows the RMSE of 3Proxies, 1P+1SP, and 1P+3SP for different disaggregation length. For all three variants, the RMSE is larger for shorter disaggregation periods. This could be because more data is available for longer periods, which is helpful to capture the true relationship between the solar generation of the target home and solar proxies. Meanwhile, we believe that the estimated weight vector for solar mixture model $\mathbf{w}$ obtained with 5 days of data is pretty close to the true values.

Selection of solar proxies: To evaluate the sensitivity of our methods to the choice of solar proxies, we randomly choose 14 target homes in Ausgrid and run 10 independent experiments with solar proxies that are randomly chosen in each experiment. Figure 3.9 shows the RMSE distribution for the 14 different target homes. It can be seen that the RMSE distributions obtained for a few target homes are wider than the rest, implying that the disaggregation method is more sensitive to the choice of solar proxies. This is because these homes are located far from the majority of homes in this dataset. Expectedly, 1P+3SP is the least sensitive variant to the choice of solar proxy because it only requires one real solar proxy and incorporates three synthetic proxies.

Table 3.3: Comparing average RMSE of disaggregated solar using different methods to initialize the weight vector $\mathbf{w}$ of the solar mixture model.

	Constant	Random	Ours
3Proxies	0.4144	0.1594	0.0590
1P+1SP	0.7544	0.3203	0.0683
1P+3SP	1.1207	0.9798	0.0649

Weight initialization: To evaluate the efficacy of our initialization method, we compare it with constant and random initialization methods. We simply set $\mathbf{w}$ to $\mathbf{1}$ for constant initialization. For random initialization, we assign random numbers in the range of $[0, 1]$ to the weights. Table 3.3 compares the results. It is evident that our weight initialization method can significantly

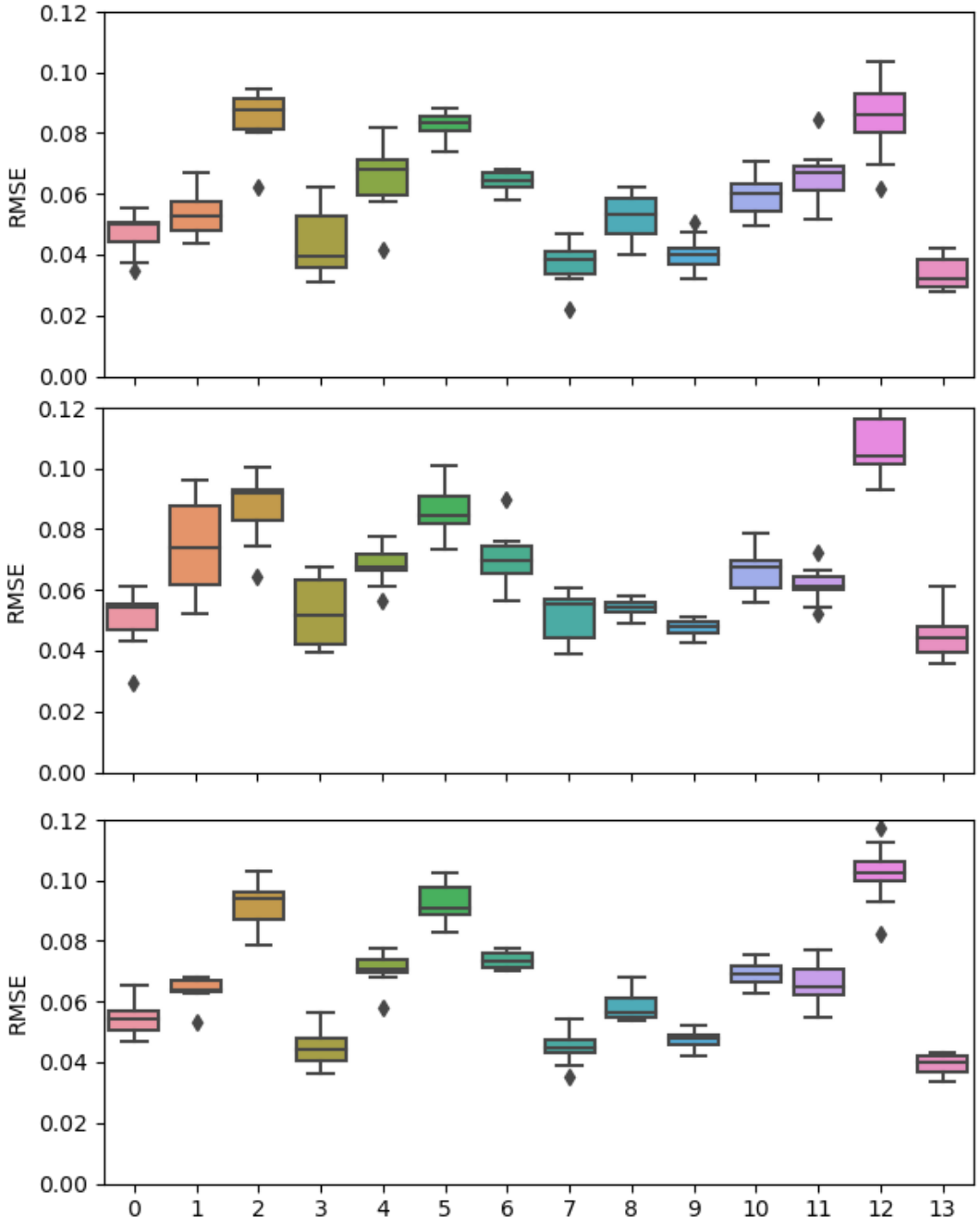

Figure 3.9: The distribution of RMSE values obtained using different choices for solar proxies used in solar mixture model. The top plot shows the results from 3Proxies, the middle plot shows the results from 1P+1SP, and the bottom one shows the results from 1P+3SP. The x-axis indicates the home index.

increase the accuracy of solar disaggregation, especially when we use only one real solar proxy (i.e., 1P+1SP and 1P+3SP). We attribute this to the fact that we take into account the PV system deployment characteristics estimated by

SolarTK.

3.4.3 NILM Performance

In recent years, more and more research groups and companies have been focusing on developing advanced NILM techniques. However, to our knowledge, all the NILM methods are supposed to be applied to household demand which does not contain behind-the-meter solar generation. Thus, it indicates the need to disaggregate solar power from net meter data before trying to separate the household demand into the constituent appliances. In this subsection, we are going to investigate the question that how much will the performance of NILM techniques be affected for customers with PV systems, if we directly apply them into metered net load data instead of the disaggregated home demand. For the purpose of this study, We use 1-minute resolution data from Pecan Street [24], since this dataset has both solar generation and individual appliance consumption data. we select 6 homes from the dataset that have both solar generation and individual appliance consumption data, and apply three benchmark NILM techniques, namely FHMM [19], Seq2Point [61], and DAE [31]. These techniques are implement[4]. Following the recommendation of [22], which explored the impact of the temporal resolution of data on the accuracy of NILM methods, we use data with 1-minute resolution.

We evaluate the performance of these 3 NILM methods in disaggregating the loads of 7 appliances, including the washing machine, microwave, air conditioner, furnace, fridge, dryer and dish washer, in each of the 6 homes. Since a dryer is not present in 4 of these homes, we only report the results for the remaining 2 homes for this appliance. We train appliance models using real home load and individual appliance load data collected between June 1 and June 22, 2018. We then calculate the error of disaggregating each appliance's load in the test data (from June 23 to June 30, 2018) with 5 different sets of input data, including the true home load, the net load (i.e., home load - BTM solar generation), and 3 versions of the disaggregated home load obtained by applying our disaggregation method (1P+3SP), and the two baseline methods described earlier.

Figure 3.10 shows the average RMSE for each appliance and the overall RMSE for all appliances in these homes. Two important observations can be made. First, solar disaggregation will improve the overall NILM accuracy but different appliances are affected to a different extent. The overall RMSE for all appliances will be 0.446 if we directly apply Seq2Point (the best performing NILM method) on the net load data. However, the RMSE will be 0.150 if we apply it to the disaggregated home load estimated by 1P+3SP, an impressive 66.2% improvement in disaggregation accuracy. We also observed 52.3% and 22.0% improvements for DAE and FHMM methods, respectively. Among all appliances, the air conditioner shows the most significant improvement in accuracy, while the disaggregation accuracy of the washing machine, dryer, microwave, and dish washer does not exhibit a statistically significant change. This may be due to the fact that these appliances are usually used after the sunset, when the net load is equal to the home load, while the air conditioner is used throughout the day. It is also worth mentioning that the fridge yields quite similar performance for all 5 different types of input data using the 3 NILM techniques. Our hypothesis is that this is because the fridge has a distinct power consumption pattern that is easier to detect.

Our second observation is that a higher accuracy in solar disaggregation leads to a better NILM performance, especially for appliances with more variable power usage patterns (e.g., the air conditioner). The overall RMSE of Seq2Point when it runs on the disaggregated home load obtained by the 1P+3SP method is 22.3% and 9.7% lower than when it runs on the disaggregated home load obtained by applying Baseline 1 and Baseline 2, respectively. Among the 7 appliances, the NILM performance improvement achieved by our method over the two baselines is particularly noticeable for air conditioner, which is the most power-hungry appliance in our study.

From the results depicted in Figure 3.10 it is clear that Seq2Point yields a better performance than the other 2 NILM methods. To further study the effect of solar disaggregation on the the performance of NILM, we compare the air conditioning load obtained by applying Seq2Point to the net load, true home load, and disaggregated home load using our 1P+3SP method in

Figure 3.11(A). We also show the true air conditioning load as a point of reference. We can see that the error of directly applying Seq2Point to the net load data is specially high around noon which solar generation is usually at its peak. Figure 3.11(B) compares the air conditioner load obtained by applying Seq2Point to the home load disaggregated by 1P+3SP and the 2 baselines. It can be seen that among the three solar disaggregation methods, our method enables tracking the true air conditioner's demand more closely.

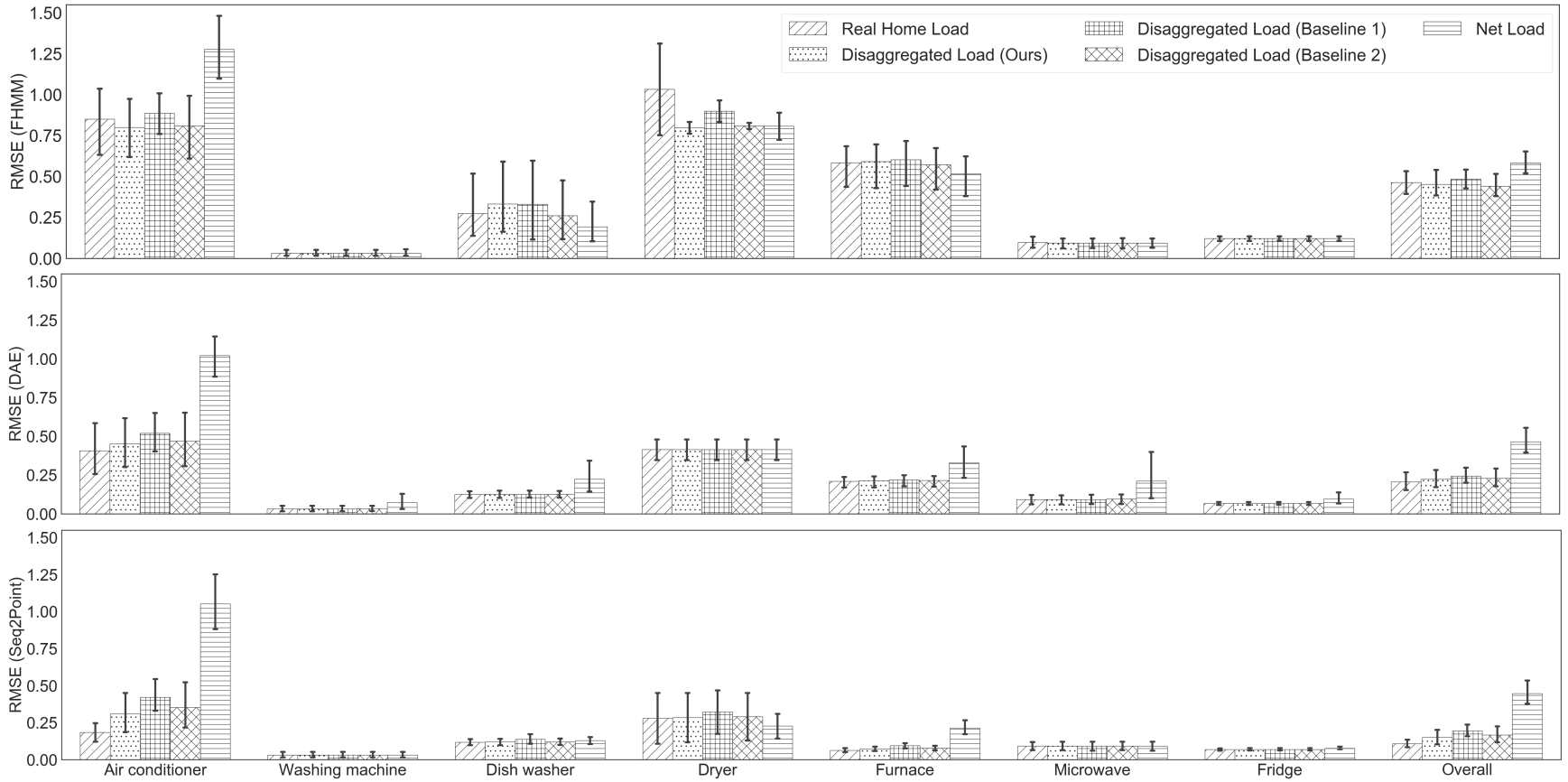

Figure 3.10: Average RMSE of each appliance among all selected homes. The top plot shows the disaggregation performance of FHMM, the middle plot shows the performance of DAE, and the bottom one shows the performance of Seq2Point. Error bars show the 95% confidence interval.

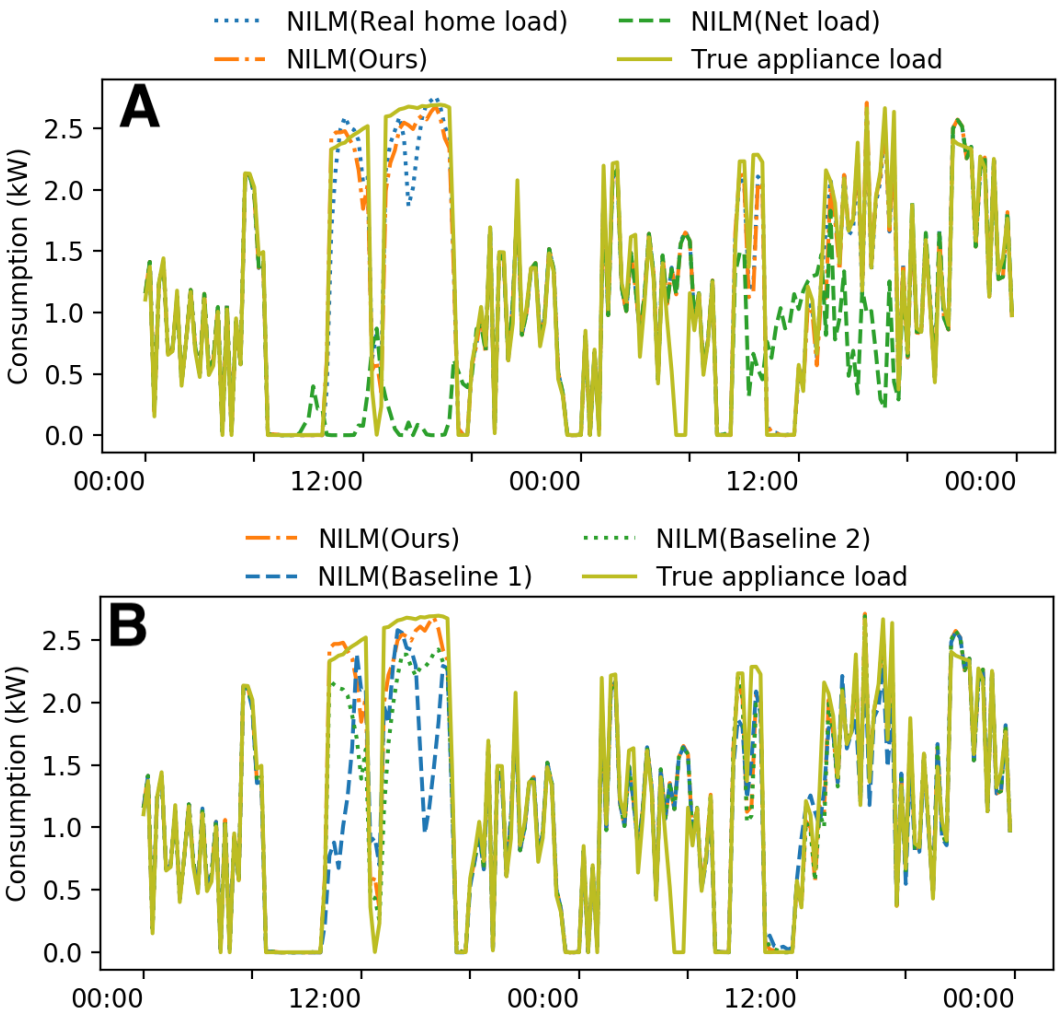

Figure 3.11: Comparison between the true and estimated air conditioner (AC) loads. The top plot shows the results of running Seq2Point on real home load, net load, and the home load disaggregated by our method (1P+3SP). The bottom plot shows the results of running Seq2Point on the home load disaggregated by our method (1P+3SP) and 2 baselines.

Chapter 4

Solar Disaggregation with Battery

In this chapter, we extend the solar disaggregation method described in Chapter 3 by considering BTM battery storage. Section 4.1 describes the problem formulation in the presence of latent battery storage and outlines the assumptions we make. Section 4.2 introduces the disaggregation algorithm, initialization techniques, and models used in this algorithm. Then Section 4.3 describes the battery control strategy, followed by the description of a baseline method. Finally, Section 4.4 shows the results in terms of disaggregation performance and discusses the sensitivity of our method to BTM battery operation strategy and battery capacity.

4.1 Problem Definition

Our objective here is to decompose the net load into three major components rather than individual appliance loads. These components are the aggregate home load, solar generation, and battery charge and discharge activities. Similar to solar disaggregation without battery, this problem must be solved in an unsupervised fashion.

4.1.1 Notation and Preliminaries

Let $\mathbf{y} \in \mathbb{R}^T$ be a vector that collects measurements of a customer's net load in T successive half-hourly intervals, Let $\hat{\boldsymbol{\ell}} \succeq 0$, $\hat{\mathbf{s}} \succeq 0$, and $\hat{\mathbf{b}}$ be vectors in $\mathbb{R}^T$

that represent respectively the estimated amount of aggregate home load, solar generation, and battery power for the same customer in these intervals. The sign of $\hat{\mathbf{b}}(t)$ indicates if the battery is being charged (negative) or discharged (positive) in interval t. When a solar-plus-battery system is installed BTM, the law of conservation of energy yields a *balance equation*: $\mathbf{y} = \hat{\boldsymbol{\ell}} - \hat{\mathbf{s}} - \hat{\mathbf{b}}$, where the LHS is the quantity measured by a smart meter.

4.1.2 Assumptions

We make similar assumptions to those made in the previous chapter. Firstly, we assume that the electric utility can only use the net meter data and approximate location of a customer, e.g., as indicated by the first segment of their postal code, for the purpose of solar disaggregation. Secondly, we postulate that the utility does not know the deployment characteristics of the BTM PV system, including its size, orientation, tilt, and temperature coefficient. Similarly, the capacity, peak power, and control strategy of the BTM battery are not provided to the utility. Thirdly, we assume there is at least one separately metered solar PV installation in the same city or district as our target home.

Lastly, we also assume there is a couple of dozen homes, which neither installed PV panels nor battery and are located in the same city or district as the target customer. Hence, the net load of each of these customers represents their aggregate household demand at any given time. This is not a strong assumption because the vast majority of homes fall under this category today and the utility can take a stratified sample of homes with different sizes and verify that they do not have BTM DER. We use the net load of these homes to approximate the target customer's home load.

4.2 Methodology

Similar to the solar disaggregation method we developed in Chapter 3 for customers who installed just PV systems, for the customers with solar-plus-battery installations, we also solve the disaggregation problem in an iterative way, but this time using a different load model and an additional battery model

Algorithm 2: SolarDisaggregationWithBattery($\mathbf{y}, \mathbf{X}^S, \mathbf{X}^L, \mathbf{X}^A$)

Input : Net load of target customer: $\mathbf{y} \in \mathbb{R}^T$
Proxy measurements from K_s PV sites: $\mathbf{X}^S \in \mathbb{R}^{T \times K_s}$
Load measurements from K_ℓ homes: $\mathbf{X}^L \in \mathbb{R}^{T \times K_\ell}$
Ambient features: $\mathbf{X}^A$

Output: Major load components: $\hat{\mathbf{s}}$, $\hat{\boldsymbol{\ell}}$, $\hat{\mathbf{b}}$; Weights: $\mathbf{w}$

// Initialization step

// First run disaggregation without battery

$\mathbf{s}^0$, $\mathbf{w}^0 \leftarrow$ SolarDisaggregationWithoutBattery($\mathbf{y}, \mathbf{X}^S, \mathbf{X}^A$)

$\boldsymbol{\ell}^0 \leftarrow$ InitLoad($\mathbf{y}, \mathbf{s}^0, \mathbf{X}^L$)

$\mathbf{b}^0, \boldsymbol{\theta}^0 \leftarrow \boldsymbol{\ell}^0 - \mathbf{s}^0 - \mathbf{y}$, $\mathbf{0}$

// Disaggregation step

do

  do

    $\boldsymbol{\ell}'^j \leftarrow$ UpdateLoad($\mathbf{s}^i + \mathbf{b}'^j + \mathbf{y}, \mathbf{b}'^j, \mathbf{X}^L$)

    $\mathbf{b}'^j, \boldsymbol{\theta}^j \leftarrow$ UpdateBattery($\boldsymbol{\ell}'^j - \mathbf{s}^i - \mathbf{y}$)

  while ($j < MaxIter$ ***and*** $\|\boldsymbol{\theta}^j - \boldsymbol{\theta}^{j-1}\| > \epsilon_2$)

  $\boldsymbol{\ell}^i, \mathbf{b}^i \leftarrow \boldsymbol{\ell}'^j, \mathbf{b}'^j$

  $\mathbf{s}^i, \mathbf{w}^i \leftarrow$ UpdateSolar($\boldsymbol{\ell}^i - \mathbf{b}^i - \mathbf{y}, \mathbf{X}^S$)

while ($i < MaxIter$ ***and*** $\|\boldsymbol{w}^i - \boldsymbol{w}^{i-1}\| > \epsilon_1$)

that we describe in Section 4.2.1.

Before applying any solar disaggregation method, we need to identify the type of customers since we use different disaggregation methods for PV customers with and without installations of BTM battery. The utility can develop a binary classification model based on historical net meter data or simply apply a clustering technique[1]. Once they are identified, the utility apply the corresponding disaggregation algorithms (i.e., Algorithm 1 and Algorithm 2) for the respective customers.

The proposed algorithm (Algorithm 2) consists of two steps: (1) initializing each latent component, and (2) updating the components iteratively until convergence.

In the first step, we start off with finding an initial estimate for solar generation. We do this by solving the solar disaggregation problem assuming the

[1]A method for identifying customers with BTM PV systems by inspecting their net meter data has been proposed in [13]. This method, with some modification, can be used to identify customers with solar-plus-battery installations.

battery is one of the home appliances, thus its charge and discharge activities are incorporated in the aggregate home load. This is done by directly calling *SolarDisaggregationWithoutBattery* described in Algorithm 1 (Section 3.2.2). We found empirically that the initial solar generation estimate found in this manner is slightly better than directly using the initial estimate returned by the InitSolar function described in 3.2.2, thereby speeding up the convergence of our algorithm. Next, an initial estimate of the aggregate home load is obtained using the load initialization method described in Section 4.2.2 (Line 2), and an initial estimate of the battery power contribution is found by applying the balance equation (Line 3). In the next step (Lines 5-10) we refine the load estimates of the 3 major BTM components one at a time in every iteration, until the parameters of our models converge. Note that instead of putting the 3 update steps in the same loop, we use nested loops and refine the solar estimate only in the outer loop. This is because the initial estimate of solar generation is relatively more accurate than the other two components, hence it does not need to be updated frequently. In the inner loop, we fix the solar generation estimate and refine the estimates of aggregate home load and battery power contribution sequentially. This is done through the use of the models described in Section 4.2.1 (Lines 6-7). Once we break out of the inner loop, we recalculate the solar power by subtracting the estimates of aggregate home load and battery power from the net load. The remainder is used to update the weights of the solar mixture model and refine the solar generation estimate (Line 10). The outer loop terminates when these weights converge or the maximum number of iterations is reached (Line 11).

4.2.1 Modelling Latent Components

We now explain the details of the BTM component models used in Algorithm 2 and discuss how the model parameters are updated in each iteration.

Solar mixture model: We use the same solar mixture model described in Section 3.2.1, which utilizes a mixture of proxy measurements from nearby PV systems to approximate the solar power generated by the target home's PV system.

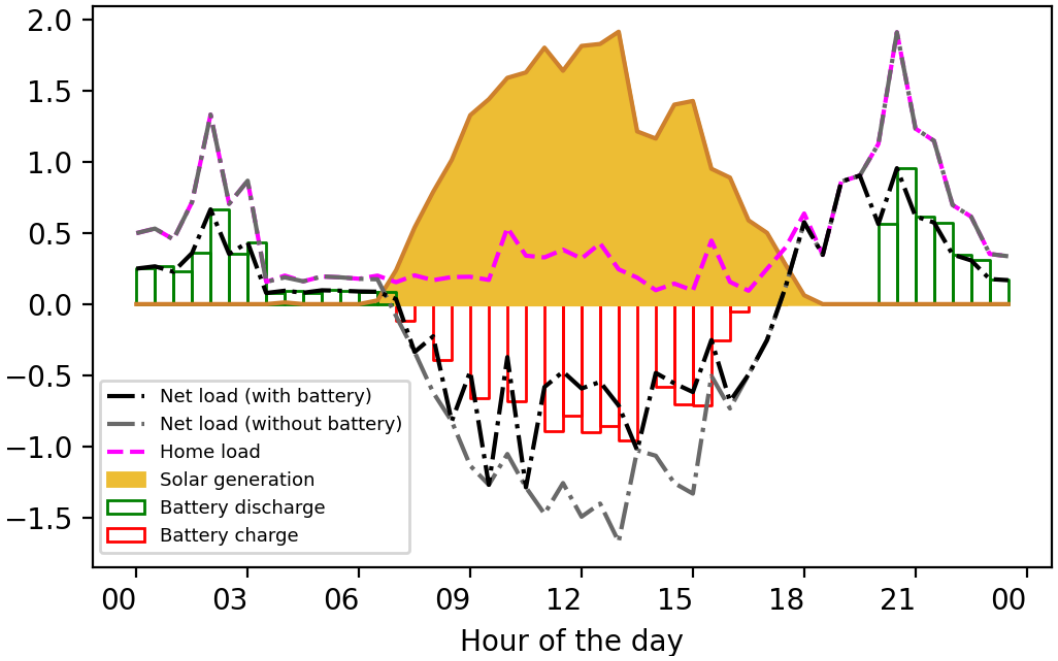

Figure 4.1: A sample customer's load curves (avg. power in 30-min intervals) over the course of a day with and without battery.

We call the UpdateSolar($\mathbf{s}, \mathbf{X}^S$) function in every iteration to update the weight vector of the solar mixture model. The first argument of this function is our current estimate of solar generation $\mathbf{s}^i = \boldsymbol{\ell}^i - \mathbf{b}^i - \mathbf{y}$. The second argument is the matrix of real and synthetic proxy measurements in T intervals, denoted $\mathbf{X}^S$. We solve the optimization problem below to update the weight vector, $\mathbf{w}$.

$$\min_{\mathbf{w} \geq 0} \quad \|\mathbf{s}^i - \mathbf{X}^S \mathbf{w}\|_2^2 + \lambda \|\mathbf{w}\|_1 \tag{4.1}$$

Let $\mathbf{w}^*$ be the optimal solution of the above optimization problem. The refined estimate of the target home's solar generation is $\mathbf{s}^i = \mathbf{X}^S \mathbf{w}^*$.

Note that the L_1 regularization is used here for two reasons. First, it induces sparsity in the weight vector, weeding out proxies with an orientation angle that is too different from that of the target home's PV system. Second, it prevents the estimates of solar generation and aggregate home load from growing unbounded together, which can happen while they still satisfy the balance equation: $\mathbf{y} = \hat{\boldsymbol{\ell}} - \hat{\mathbf{s}} - \hat{\mathbf{b}}$ because they have opposite signs.

Home load model: Given the current load estimation $\boldsymbol{\ell}'^j = \mathbf{s}^i + \mathbf{b}'^j + \mathbf{y}$,

we use a different load model to update this estimation for the customers with installations of BTM batteries.

Specifically, we use a load mixture model similar to the solar mixture model. This linear model relates the aggregate home load of neighbouring homes to the aggregate home load of the target home: $\boldsymbol{\ell} = \mathbf{X}^L \boldsymbol{\mu}$. The use of this mixture model, instead of a random forest regressor described in Section 3.2.1, is motivated by the fact that due to battery operation, the net load does not contain sufficient useful information at nighttime to extract the home load, which is evident in Figure 4.1. This prevents us from using the random forest regression model to determine the home load from environmental data.

When a BTM battery is installed, we solve the optimization problem below to refine the current load estimate $\boldsymbol{\ell}^i$ and update its weight vector $\boldsymbol{\mu}$.

$$\begin{aligned} \min_{\boldsymbol{\mu} \succeq 0} \quad & \|\boldsymbol{\ell}'^j - \hat{\boldsymbol{\ell}}\|_2^2 + \lambda \|\mathbf{A}(\boldsymbol{\ell}'^j - \mathbf{b}'^j - \hat{\boldsymbol{\ell}})\|_2^2 \\ \text{s.t.} \quad & \hat{\boldsymbol{\ell}}(d) = \mathbf{X}^L \boldsymbol{\mu}(d), \quad \forall d \in \{1, ..., D\} \end{aligned} \tag{4.2}$$

$$\mathbf{A} = \begin{bmatrix} 1 & \dots & 1 & \dots & 0 & \dots & 0 \\ 0 & \dots & 0 & \dots & 0 & \dots & 0 \\ \vdots & \vdots & \vdots & \vdots & \vdots & \vdots & \vdots \\ 0 & \dots & 0 & \dots & \underbrace{1}_{\text{indexes corresponding to interval in day D}} & \dots & 1 \end{bmatrix},$$

where $\hat{\boldsymbol{\ell}}(d)$ and $\boldsymbol{\mu}(d)$ are vectors that represent $\hat{\boldsymbol{\ell}}$ and $\boldsymbol{\mu}$ on day d, respectively, and D is the total number of days for which we solve the problem. $\mathbf{A} \in \mathbb{R}^{D \times T}$ is a binary matrix that sums a signal over all the intervals of each day. We use this matrix to enforce the constraint that the battery state of charge (SoC) at the beginning of the day must be roughly equal to its SoC at the end of the day; this can be expressed as follows: $\mathbf{Ab} \approx \mathbf{0}$.

Battery model: Given the current estimate of battery charge and discharge activities $\mathbf{b}'^j = \boldsymbol{\ell}'^j - \mathbf{s}^i - \mathbf{y}$, we use a general model to update this estimation without relying on the knowledge of its control strategy, peak power, and capacity. The rationale is that utilities have no way to tell what kind of battery is installed and how it is controlled by the customer, e.g., if it is used to perform tariff optimization, shave the peak demand, or maximize

self-consumption of solar power generated on-site. Solving the disaggregation problem without knowing these parameters is indeed a challenging task.

We split a day into K time slots of equal length, denoted T_b, and model charge and discharge activities of the battery in each time slot as the weighted sum of sine and cosine waves with period of T_b. Note that K is an adjustable hyper-parameter; we found empirically that setting it to 3 ($T_b = 8hr$) yields the best result. We assume each quadrant of the sine and cosine waves in a time slot is multiplied by a different weight factor, yielding 12 weight factors for the sine wave and 12 weight factors for the cosine wave for one day. The smoothness of sine and cosine functions makes them excellent candidates to characterize battery operation which is not expected to change abruptly on a timescale of half an hour as controllers are wary of the battery lifespan. Next we calculate the weight factors by solving the problem below.

$$\begin{aligned} \min_{\boldsymbol{\alpha},\boldsymbol{\beta}} \quad & \|\mathbf{b}'^{j} - \hat{\mathbf{b}}\|_2^2 + \lambda \|\mathbf{A}\hat{\mathbf{b}}\|_2^2 \\ \text{s.t.} \quad & \hat{\mathbf{b}}(t) = \boldsymbol{\alpha}(t)\sin(\frac{2\pi t}{T_b}) + \boldsymbol{\beta}(t)\cos(\frac{2\pi t}{T_b}), \quad \forall t \in \{1, ..., T\} \\ & |\hat{\mathbf{b}}(t)| \leq \max(-\mathbf{b}'^{j}), \quad \forall t \in \{1, ..., T\} \end{aligned} \tag{4.3}$$

where $\boldsymbol{\alpha}(t)$ and $\boldsymbol{\beta}(t)$ are the weight factors of sin and cos at time t, respectively. If t_1 and t_2 fall into the same quadrant, $\boldsymbol{\alpha}(t_1)$ will be equal to $\boldsymbol{\alpha}(t_2)$. The same rule applies to $\boldsymbol{\beta}$. The vector $\boldsymbol{\theta} = [\boldsymbol{\alpha}, \boldsymbol{\beta}]$ collects all weight factors. Note that $\max(-\mathbf{b}'^{j})$ is the maximum amount of energy that can be charged into the battery in a half hour time slot according to the current estimate $\mathbf{b}'^{j}$. Although the battery's peak charge and discharge powers are the same, we use $\max(-\mathbf{b}'^{j})$ rather than $\max(\mathbf{b}'^{j})$ because our experiments suggested that charge activities are usually estimated more accurately than discharge activities. This can be attributed to the fact that a relatively accurate estimate of solar generation is obtained in the first few iterations and that charge activities often take place when there is solar generation and aggregate home load is small. Note that estimating this peak power accurately is essential to improve the overall accuracy of our disaggregation method.

4.2.2 Initialization

For the customers with BTM battery systems, the first step of our disaggregation method is initializing the weights of the solar model, and the aggregate home load when a battery is installed behind the meter. A good initialization can boost the performance of the disaggregation method while reducing its convergence time. For solar model initialization, we treat home battery as one of the home appliances and directly apply *SolarDisaggregationWithoutBattery* function in Algorithm 1 to obtain the initial estimate of solar generation.

Load initialization: InitLoad($\mathbf{y}, \mathbf{s}^0, \mathbf{X}^L$)

For the customers with BTM batteries, we need to find the initial weights of the load mixture model. To this end, after obtaining the initial solar generation estimate $\mathbf{s}^0$, we enforce the constraint that the battery SoC at the beginning of the day must be roughly equal to the SoC at the end of the day: $\mathbf{A}\boldsymbol{\ell}^0 \approx \mathbf{A}(\mathbf{y} + \mathbf{s}^0)$. Therefore, solving the following optimization problem yields the initial estimate of the load mixture model weight:

$$\min_{\boldsymbol{\mu} \succeq 0} \quad \|\mathbf{A}\mathbf{X}^L\boldsymbol{\mu} - \mathbf{A}(\mathbf{y} + \mathbf{s}^0)\|_2^2$$

Once $\boldsymbol{\mu}^*$ is found, the initial home load estimate of the target home can be calculated as follows $\boldsymbol{\ell}^0 = \mathbf{X}^L\boldsymbol{\mu}^*$.

4.3 Evaluation

We use the same dataset (i.e., Ausgrid [2]) as we use for the experiments in Section 3.3 to measure the performance of our disaggregation method for the customers with BTM battery system. Since we use the same solar mixture model, we can still implement and benchmark our disaggregation method with different solar proxy settings. In these experiments, we compare the two main proxy settings (3Proxies and 1P+3SP) introduced in Section 3.3.2.

4.3.1 Battery Control Strategies

Since the Ausgrid dataset does not contain any home with a BTM battery (or they are not identified in the dataset), we simulate battery activities using

System Advisor Model (SAM) software [16]. Specifically, we feed the actual measurements of a home's solar generation and home load to SAM to obtain the battery operation assuming that it is a Nickel Manganese Cobalt Oxide (NMC) lithium-ion cell. Unless otherwise stated, we set the battery capacity to 6.4kWh, its maximum charge/discharge power to 2kW, and the default control strategy to peak shaving (PS) [16]. This strategy uses a 24-hour look ahead for home load and PV generation (i.e., assumes accurate forecasts for the next day) to reduce the peak demand of the household. To test the robustness of our method to different battery control strategies, we also simulate the price signal forecast [38] dispatch option, which performs tariff optimization (TO) to minimize the electricity bill and battery degradation cost, for each home using the same battery capacity and power rating. This strategy utilizes day-ahead PV and load forecasts, battery degradation data, and time-of-use (TOU) rates. The TOU rates are collected from the Ausgrid website to keep it consistent with the home load data. Figure 4.2 shows the daily battery charge/discharge activity of one home over a month when the battery is controlled using the two hypothetical strategies. It can be seen that the control strategy affects charge and discharge times of the battery. For instance, by utilizing price information, the tariff optimization strategy schedules more charge activities in early morning hours than the peak shaving strategy; this is because the electricity price is cheaper during that time.

4.3.2 Baseline

To compare our disaggregation method for the customers with BTM batteries, we choose the baseline method proposed in [14], which also takes the BTM batteries into the consideration in their disaggregation algorithm. We label this baseline as "Baseline 3". Note that this baseline uses solar and load models that are similar to ours except that they approximate the battery operation as a sine wave with a single weight factor for each day. For a fair comparison, we select the same solar proxies in the solar model and use the same neighboring homes to approximate the home load in each experiment. We also compare our method with theirs using synthetic proxies (i.e., 1P+3SP),

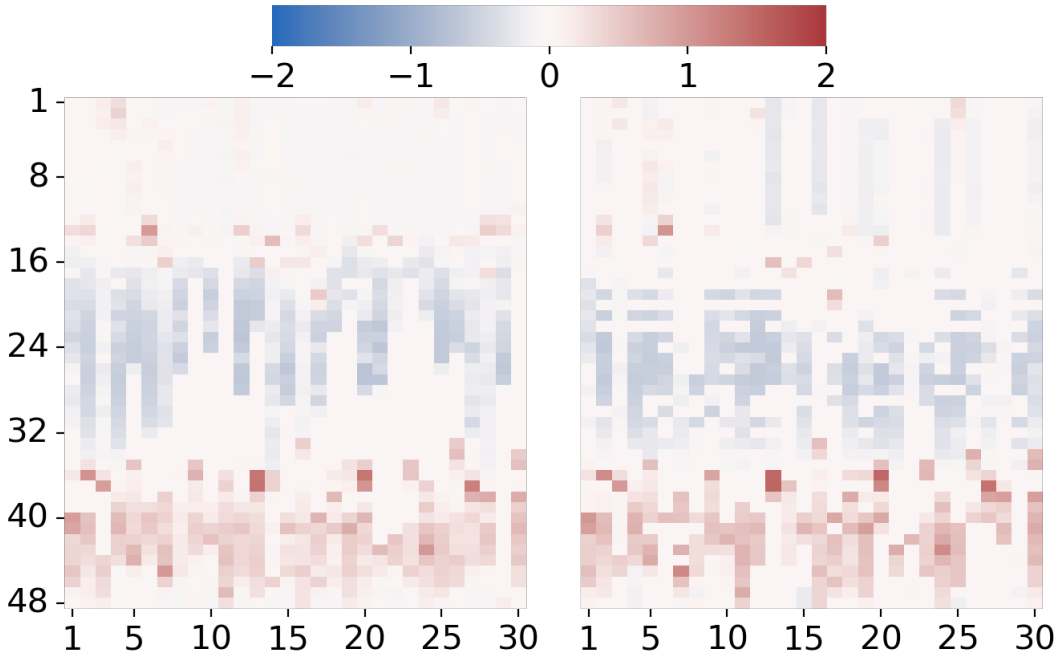

Figure 4.2: The heat map of the two distinct battery control strategies, peak shaving (PS) on the left and tariff optimization (TO) on the right, over 30 days for one customer. The x-axis shows day of the month. The y-axis indicates the 30-minute intervals in one day, so 1 refers to the first interval of a day and 48 refers to the last interval of that day. Negative (positive) values indicate the power (in kW) charged into (discharged from) the battery in respective intervals.

although synthetic proxies are not used in their work. Since Baseline 3 uses the same solar mixture model as ours, their method can benefit from using synthetic solar proxies, the idea we propose in this thesis. Additionally, to show that solar disaggregation methods that do not consider latent battery storage have an inferior performance in the presence of BTM batteries, we also use Baseline 1 and 2 described in Section 3.3.3 to disaggregate solar generation. These two baselines treat the battery as one of the home appliances.

4.4 Experimental Results

We conduct a set of experiment to compare our disaggregation method in the existence of BTM batteries. Since meter readings from customers with battery installations are not included in our dataset, we use SAM to simulate battery charge and discharge activities for each customer and superpose this on their

net load as described in Section 4.3.1.

We first evaluate the disaggregation performance of our methods using the two metrics (RMSE and nRMSE) introduced in Section 3.3.4. The performance evaluation includes battery peak power estimation, solar generation and home load disaggregation accuracy. We then analyze the sensitivity of our methods to different battery control strategies and different battery capacities.

4.4.1 Disaggregation Performance

Solving this disaggregation problem in an unsupervised fashion without knowing physical characteristics of DER is indeed quite difficult. We consider the two best solar proxy settings, i.e., 3Proxies and 1P+3SP, to compare our method with Baseline 3. It should be noted that Reference [14], which is Baseline 3, does not consider the use of synthetic proxies. Instead, it uses data from 15 real proxies for each home. Yet, we implement this method with both real and synthetic proxies for fair comparison with our work. Moreover, we compare the solar estimation accuracy with Baseline 1 and Baseline 2 introduced in Section 3.3.3 to explore how the presence of BTM battery could affect the performance of these methods that are not originally designed to work when other types of DER are installed behind the meter. Recall that when a BTM battery is installed, our disaggregation method relies on a mixture model to approximate the load of the target home given the loads of a number of neighboring homes. To this end, for each target home, we randomly choose 20 homes in the Ausgrid dataset that do not have a PV system or battery. Measurements from these homes are used to build the load model.

Estimating the peak charge/discharge power: We now discuss how accurately we can estimate the peak charge or discharge power of the battery. Since the peak charge and discharge rates of a lithium-ion battery are normally equal, we refer to both as the battery's *peak power*. We argue that the more accurate our estimate of the peak power becomes, the better we could disaggregate solar generation as it is used in the second constraint of (4.3).

We note that, for various reasons, the battery operation signal simulated by SAM may never include the preset peak power, i.e., 2kW. In that case, we

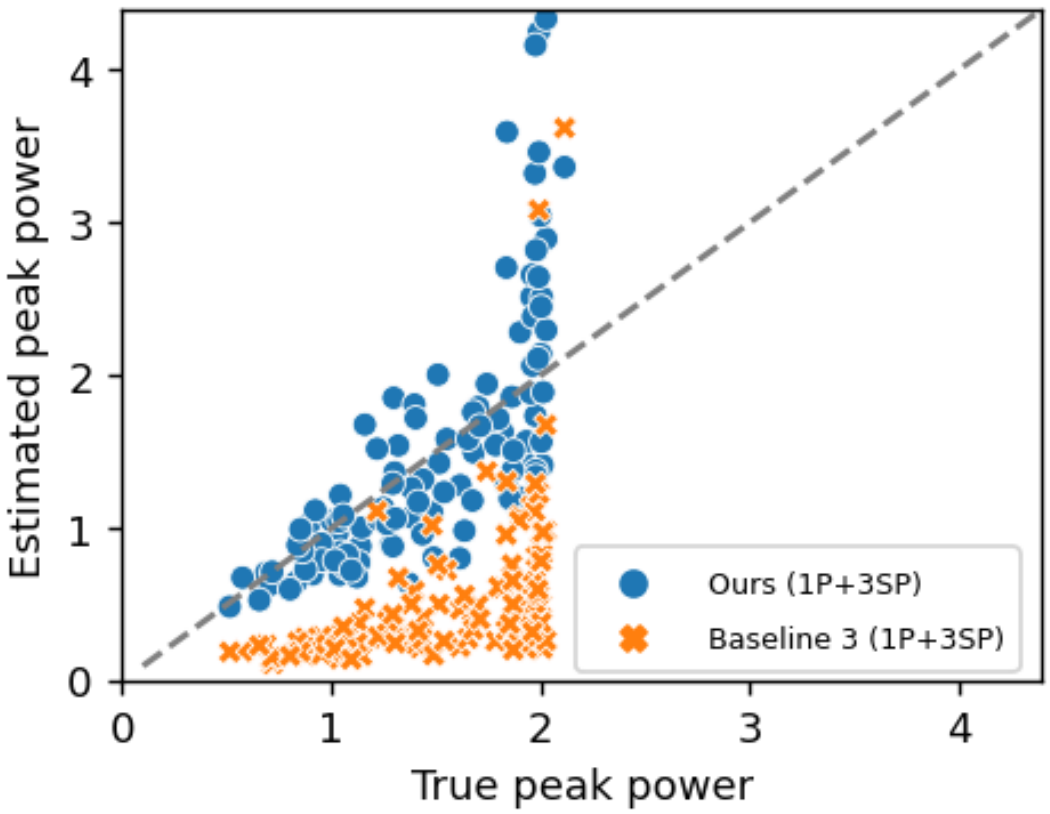

Figure 4.3: Comparison of true and estimated battery peak charge/discharge power using our method and Baseline 3 in the 1P+3SP setting. We assume each battery system has the same peak charge and discharge power. The dashed line shows $y = x$.

treat the maximum power that was simulated by SAM as the true peak power. As shown in Figure 4.3, the peak power estimated by our method is closer to the true peak power of the battery compared to Baseline 3. Overall the mean absolute error of the estimated peak power with respect to the real peak power is 0.4092 using our method (1P+3SP), while it is 1.0322 for Baseline 3 in the same solar proxy setting.

Solar disaggregation accuracy: Table 4.1 and Table 4.2 show the average RMSE and nRMSE of solar generation and home load estimation across all customers in two seasons, considering two battery control strategies. We first look at the peak shaving (PS) strategy. It can be readily seen that our method outperforms Baseline 3 in both seasons with 1P+3SP and 3Proxies solar proxy settings, reducing the RMSE of solar generation by 8.67% and 12.73% on aver-

Table 4.1: Comparison of disaggregation methods for the customers with BTM battery systems using two different battery operation strategies. Each cell contains average RMSE across all customers.

		Summer		Winter	
Method	Ctrl	Solar	Load	Solar	Load
Ours (1P+3SP)	PS	0.0740	0.2229	0.0702	0.2698
Baseline 3 (1P+3SP)	PS	0.0777	0.2397	0.0801	0.2937
Ours (3Proxies)	PS	0.0690	0.2232	0.0626	0.2704
Baseline 3 (3Proxies)	PS	0.0748	0.2402	0.0758	0.2915
Ours (1P+3SP)	TO	0.0825	0.2229	0.0766	0.2682
Baseline 3 (1P+3SP)	TO	0.0873	0.2412	0.0793	0.2948
Ours (3Proxies)	TO	0.0772	0.2229	0.0710	0.2694
Baseline 3 (3Proxies)	TO	0.0834	0.2417	0.0759	0.2930

The second column indicates the battery control strategy. PS stands for peak shaving with one-day look ahead and TO stands for tariff optimization.

Table 4.2: Comparison of disaggregation methods for the customers with BTM battery systems using two different battery operation strategies. Each cell contains average nRMSE across all customers.

		Summer		Winter	
Method	Ctrl	Solar	Load	Solar	Load
Ours (1P+3SP)	PS	0.583	0.785	0.851	0.856
Baseline 3 (1P+3SP)	PS	0.605	0.844	0.983	0.936
Ours (3Proxies)	PS	0.540	0.786	0.771	0.858
Baseline 3 (3Proxies)	PS	0.582	0.846	0.931	0.930
Ours (1P+3SP)	TO	0.658	0.787	0.942	0.857
Baseline 3 (1P+3SP)	TO	0.681	0.853	0.973	0.948
Ours (3Proxies)	TO	0.598	0.788	0.885	0.861
Baseline 3 (3Proxies)	TO	0.644	0.855	0.920	0.943

The second column indicates the battery control strategy. PS stands for peak shaving with one-day look ahead and TO stands for tariff optimization.

age, respectively. The same observation can be made about the load estimation accuracy in both seasons. From Figure 4.4 we can conclude that Baseline 3 fails to capture most of the variations in the home load. This leads to several problems should the estimate home load be further decomposed into individual appliance loads through the application of a non-intrusive load monitoring technique [12]. We attribute this to the fact that this baseline attempts to fit a single sine wave to the battery operation signal.

Meanwhile, we apply Baseline 1 and Baseline 2 to disaggregate solar power from the net meter data when battery is installed behind the meter and used for peak shaving. Recall that these baselines are not capable of decomposing the net meter data into three components; thus, we pretend that battery is one of the home appliances and only decompose the net meter data into solar generation and other loads. We find that the average RMSE of solar generation using Baseline 2 is 1.2671 in summer and 0.2387 in winter, which is around 80% higher than the average RMSE of solar generation when battery was not installed (cf. Table 3.2). Interestingly, the average RMSE of solar generation using Baseline 1 is 0.0777 in summer and 0.0813 in winter. This is on par with the accuracy of Baseline 3, but still worse than our method. We believe that this is because, without battery, Baseline 1 tends to overestimate solar generation, especially in winter. Since charging the battery reduces the net load, Baseline 1 estimates improve when battery is installed. Overall, our disaggregation method can beat all baseline algorithms in both seasons regardless of what components are installed behind the meter, and can separate battery activities from home load, thereby supporting NILM applications that rely on the home load data.

4.4.2 Sensitivity Analysis

Battery control strategy: we evaluate the sensitivity of our method and Baseline 3 to the choice of the battery control strategy. Table 4.1 allows us to compare the disaggregation performance for peak shaving (PS) and tariff optimization (TO) strategies in both summer and winter. It can be seen that changing the control strategy affects the performance but the performance of

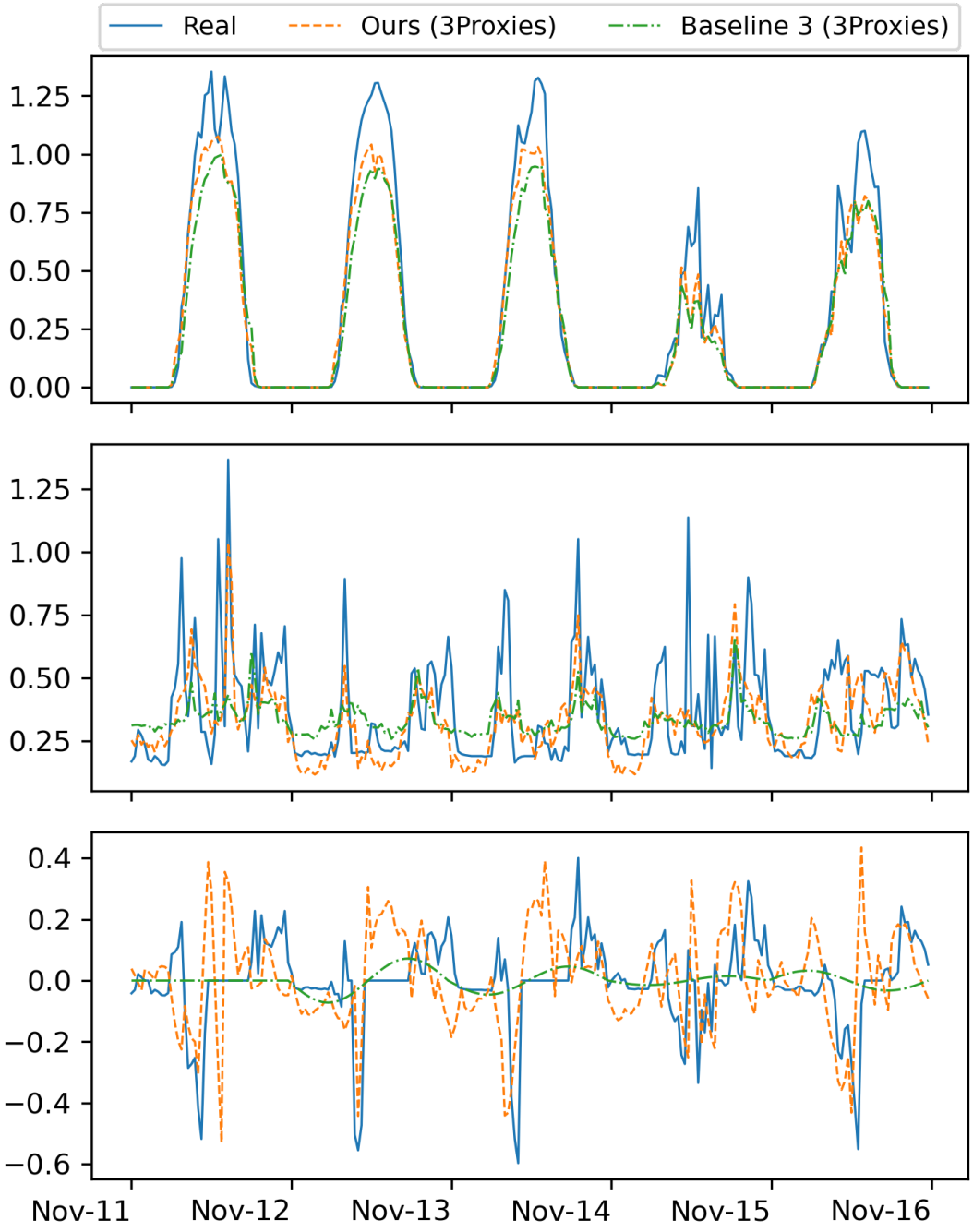

Figure 4.4: Comparison of disaggregated BTM components - solar generation (top), home load (middle) and battery operation (bottom), for a customer with a BTM battery in five days. The y-axis shows the average power (in kW) consumed or generated in a 30-min interval.

our method is still superior to Baseline 3. Notice that our method does not make any assumption about the battery control strategy adopted by the target home.

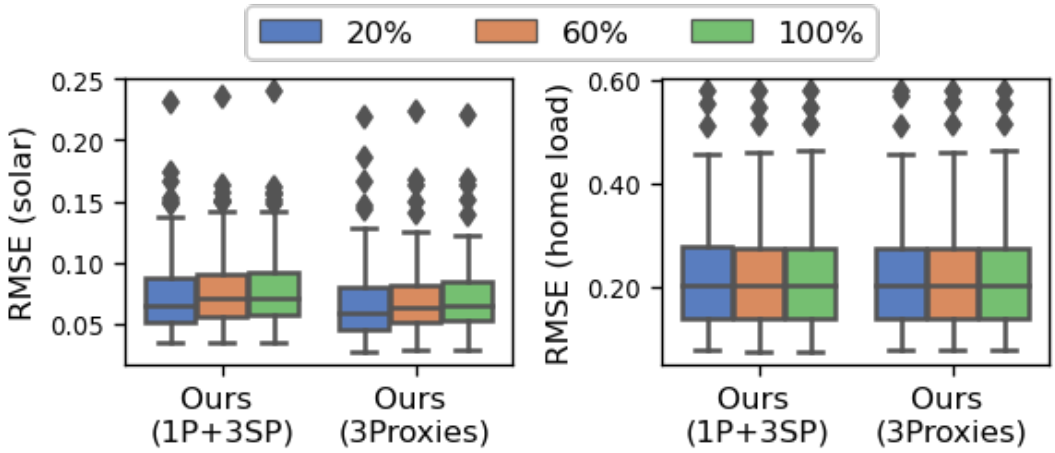

Figure 4.5: The distribution of RMSE values obtained using different battery capacities. We set the battery capacity to be 20%, 60%, and 100% of the average daily household demand. The left plot shows the accuracy of solar production estimates and the right plot shows the accuracy of home load estimates. The length of the whiskers shows 1.5 times IQR.

Effect of varying the battery capacity: We investigate the sensitivity of our result to the battery capacity. To this end, we set the battery capacity to be 20%, 60%, and 100% of the average daily household demand and re-run the disaggregation method. We choose 20% and 60% of the average daily demand because roughly speaking, for most homes, they give the capacity of commercial home batteries that are available in the market. Figure 4.5 shows the distribution of RMSE values when our method is used for disaggregation in the 1P+3SP and 3Proxies settings. As the battery capacity increases, we can see that the median of the disaggregation error increases slightly for solar generation, but this effect is less pronounced for the home load. This is expected because a bigger battery can mask some fluctuations in the net load that are deemed useful for disaggregation when solar generation is non-zero. We conclude that increasing the battery capacity could negatively affect our result but this impact is small for realistic battery capacities in the range of 5 to 15kWh.

Chapter 5

Conclusion

Solar PV generation is one of the fastest-growing renewable energy sources worldwide. High penetration of solar PV brings new challenges for the distribution system planning and operation, requiring the utilities to develop low-cost disaggregation techniques for monitoring the solar power injected into their systems. In this thesis, we first surveyed the literature on the solar disaggregation area, identified key challenges that must be overcome, and presented opportunities for improving the accuracy of disaggregation techniques. Then we studied and answered three important research questions in the solar disaggregation area under the assumption that historical disaggregated data from the target home is unavailable and the deployment characteristics of the BTM PV systems are unknown. The first question is how to disaggregate solar generation in a more data efficient way? The second question is about the accuracy of NILM techniques when they are applied to the disaggregated home load. Can we still understand which appliances are turned on and when? Finally, as more BTM batteries are expected to be installed in customers' houses, can we maintain the performance of disaggregating solar generation in the presence of BTM battery?

For the first question, we proposed an approach that entails inferring the physical characteristics from smart meter data and disaggregating solar generation using an iterative algorithm. This algorithm takes advantage of solar generation data (aka proxy measurements) from a few sites that are located in the same area as the target home, and solar generation data synthesized

using a physical PV model. We evaluated our methods with 4 different proxy settings on around 140 homes in Australia. Table 3.2 showed that the solar disaggregation accuracy is significantly improved over two state-of-the-art methods using only one real proxy along with three synthetic proxies.

For the second question, we investigated whether a more accurate disaggregation technique could lead to higher accuracy in NILM. Our results, shown in Figure 3.10, suggested that using the disaggregated home load rather than the net load data could improve the overall accuracy of three popular NILM methods.

For the third question, we extended our work and tackled the problem in the presence of a BTM battery without knowing its capacity, peak charge/discharge power, and control strategy. To our best knowledge, most state-of-the-art disaggregation methods are designed assuming that the PV system is the only type of DER installed behind the meter. For the customers with solar-plus-battery installations, we solved the solar disaggregation via an iterative method but using a different load model and an additional battery model. We evaluated our methods with 2 different proxy settings on around 140 homes in Australia. Because meter readings from customers with battery installations are not included in the dataset, we simulated the battery charge and discharge activities for each customer and superpose this on their net load. The results in Table 4.1 and Table 4.2 showed that our method can improve the performance of solar production estimation by a clear margin over a baseline that tries to model operations of the latent battery.

The research presented in this thesis has certain limitations that we plan to address in future work:

- Our disaggregation methods are not evaluated in a different climate where snow accumulation can significantly affect the output of PV systems. The snow coverage situations in solar proxies and target PV system may not only be different but also change over time. This poses a significant challenge to find the true relationship between the solar generation of the target home and solar proxies. In future work, we plan to

test our methods in winter in a country, like Canada.

- Both of our methods are designed for customer-level solar disaggregation. In addition to the net load data, feeder-level disaggregation methods benefit from data that can only be collected at a higher level of aggregation, e.g., high-resolution voltage and current phasor measurements taken at feeder head. In future work, we aim to explore how the proposed solar disaggregation technique can be used to estimate the total amount of solar power generated below a distribution transformer or in one neighbourhood.

- In Chapter 4, we evaluated our method using simulated battery activities. In reality, the batteries installed behind the customer's meter may vary in terms of make and model, operating strategy, capacity, and peak charge/discharge power. We plan to evaluate our method using data from real customers with solar-plus-battery installations. This allows us to use the operation of a real battery rather than simulating it. We also aim to study the disaggregation problem in the presence of mobile batteries, e.g., from plug-in electric vehicles.

- We investigate one source of latent flexibility (i.e., BTM energy storage) only. Nowadays, the shape of the net load can change due to other reasons, such as demand response mechanisms and smart thermostat operations. This creates problems for most data-driven solar disaggregation methods. In future work, we plan to extend our work by considering other sources of flexibility.

Despite these limitations, the work presented in this thesis makes several significant contributions in the solar disaggregation area. First, the proposed data-efficient solar disaggregation method advances the state of the art in terms of data needs and disaggregation accuracy. Second, for the first time, we have quantified the change in the accuracy of NILM techniques when they run on the disaggregated home load rather than the net load measured by a smart meter. Last but not least, the method proposed in Chapter 4 is one

of the few attempts to disaggregate solar generation from net meter data in the presence of a BTM battery. We hope that this work sets a foundation for future work on solar modelling, prediction, and disaggregation, and facilitates the development of new methods.

References

[1] O. Ardakanian, S. Keshav, and C. Rosenberg, *Integration of Renewable Generation and Elastic Loads into Distribution Grids*. 2016. DOI: 10.1007/978-3-319-39984-3.

[2] Ausgrid, *Solar home electricity data*, https://www.ausgrid.com.au/Industry/Our-Research/Data-to-share/Solar-home-electricity-data.

[3] N. Bashir *et al.*, "Solar-TK: A data-driven toolkit for solar PV performance modeling and forecasting," in *Proc. 16th International Conference on Mobile Ad Hoc and Sensor Systems (MASS)*, IEEE, 2019, pp. 456–466.

[4] N. Batra *et al.*, "Towards reproducible state-of-the-art energy disaggregation," in *Proc. 6th International Conference on Systems for Energy-Efficient Buildings, Cities, and Transportation*, ACM, 2019, pp. 193–202.

[5] J. Brown *et al.*, "Disaggregation of household solar energy generation using censored smart meter data," *Energy and Buildings*, vol. 231, p. 110 617, Nov. 2020.

[6] F. Bu *et al.*, "A time-series distribution test system based on real utility data," *2019 North American Power Symposium (NAPS)*, pp. 1–6, 2019.

[7] ——, "A data-driven game-theoretic approach for behind-the-meter pv generation disaggregation," *IEEE Transactions on Power Systems*, vol. 35, pp. 3133–3144, 2020.

[8] F. Bu, K. Dehghanpour, Y. Yuan, Z. Wang, and Y. Guo, "Disaggregating customer-level behind-the-meter pv generation using smart meter data and solar exemplars," *IEEE Transactions on Power Systems*, vol. 36, no. 6, pp. 5417–5427, 2021. DOI: 10.1109/TPWRS.2021.3074614.

[9] D. Chen and D. Irwin, "Sundance: Black-box behind-the-meter solar disaggregation," *Proc. 8th International Conference on Future Energy Systems*, pp. 45–55, 2017.

[10] D. Chen, S. Iyengar, D. Irwin, and P. Shenoy, "Sunspot: Exposing the location of anonymous solar-powered homes," in *Proceedings of the 3rd ACM International Conference on Systems for Energy-Efficient Built Environments*, ser. BuildSys '16, Palo Alto, CA, USA: ACM, 2016, pp. 85–94.

[11] X. Chen *et al.*, "Solar disaggregation: State of the art and open challenges," in *Proc. 5th International Workshop on Non-Intrusive Load Monitoring*, ACM, 2020, pp. 6–10.

[12] ——, "Disaggregating solar generation using smart meter data and proxy measurements from neighbouring sites," in *Proc. 12th ACM International Conference on Future Energy Systems*, ACM, 2021, pp. 225–230.

[13] C. M. Cheung *et al.*, "Behind-the-meter solar generation disaggregation using consumer mixture models," in *International Conference on Communications, Control, and Computing Technologies for Smart Grids*, IEEE, 2018, pp. 1–6.

[14] C. M. Cheung, S. R. Kuppannagari, R. Kannan, and V. K. Prasanna, "Disaggregation of behind-the-meter solar generation in presence of energy storage resources," in *2020 IEEE Conference on Technologies for Sustainability (SusTech)*, 2020, pp. 1–7. DOI: 10.1109/SusTech47890.2020.9150506.

[15] C. Dinesh *et al.*, "Non-intrusive load monitoring under residential solar power influx," *Applied Energy*, vol. 205, pp. 1068–1080, 2017.

[16] N. DiOrio, "An overview of the automated dispatch controller algorithms in the system advisor model (SAM)," National Renewable Energy Laboratory, Tech. Rep., 2017. [Online]. Available: https://www.nrel.gov/docs/fy18osti/68614.pdf.

[17] A. Dobos, "Pvwatts version 5 manual," Tech. Rep., 2014, Research Organization: National Renewable Energy Lab. (NREL), Golden, CO (United States).

[18] Energy Information Administration, "Annual energy outlook 2020," *US Department of Energy*, 2020.

[19] Z. Ghahramani and M. I. Jordan, "Factorial hidden markov models," *Mach. Learn.*, vol. 29, no. 2–3, pp. 245–273, 1997, ISSN: 0885-6125.

[20] G. W. Hart, "Nonintrusive appliance load monitoring," *Proceedings of the IEEE*, vol. 80, no. 12, pp. 1870–1891, 1992.

[21] J. de Hoog *et al.*, "Using satellite and aerial imagery for identification of solar PV: State of the art and research opportunities," in *Proc. 11th International Conference on Future Energy Systems*, ACM, 2020, pp. 308–313.

[22] J. Huchtkoetter *et al.*, "On the impact of temporal data resolution on the accuracy of non-intrusive load monitoring," in *Proc. 7th International Conference on Systems for Energy-Efficient Buildings, Cities, and Transportation*, ACM, 2020, pp. 270–273.

[23] I. N. E. Inc., *Zonal information*, `https://www.iso-ne.com/isoexpress/web/reports/pricing/-/tree/zone-info`.

[24] P. S. Inc., *Dataport*, `https://www.pecanstreet.org/dataport/`.

[25] Institute For Energy Research, *Hawaiians learning about the pitfalls of solar power*, `https://www.instituteforenergyresearch.org/renewable/solar/hawaiians-learning-about-the-pitfalls-of-solar-power/`, 2015.

[26] F. Kabir *et al.*, "Estimation of behind-the-meter solar generation by integrating physical with statistical models," in *2019 IEEE International Conference on Communications, Control, and Computing Technologies for Smart Grids*, 2019, pp. 1–6.

[27] F. Kabir *et al.*, "Joint estimation of behind-the-meter solar generation in a community," *IEEE Transactions on Sustainable Energy*, vol. 12, no. 1, pp. 682–694, 2021.

[28] E. Kara *et al.*, "Estimating behind-the-meter solar generation with existing measurement infrastructure: Poster abstract," in *Proc. 3rd ACM International Conference on Systems for Energy-Efficient Built Environments*, ACM, 2016, pp. 259–260.

[29] ——, "Disaggregating solar generation from feeder-level measurements," *Sustainable Energy, Grids and Networks*, vol. 13, pp. 112–121, 2018.

[30] E. C. Kara *et al.*, "Towards real-time estimation of solar generation from micro-synchrophasor measurements," *ArXiv*, vol. abs/1607.02919, 2016.

[31] J. Kelly *et al.*, "Neural NILM: Deep neural networks applied to energy disaggregation," *Proc. 2nd ACM International Conference on Embedded Systems for Energy-Efficient Built Environments*, 2015.

[32] H. Kim *et al.*, "Unsupervised disaggregation of low frequency power measurements," vol. 11, Apr. 2011, pp. 747–758.

[33] R. Kukunuri *et al.*, "Edgenilm: Towards nilm on edge devices," in *Proc. 7th International Conference on Systems for Energy-Efficient Buildings, Cities, and Transportation*, ACM, 2020, pp. 90–99.

[34] K. Li *et al.*, "Capacity and output power estimation approach of individual behind-the-meter distributed photovoltaic system for demand response baseline estimation," *Applied Energy*, vol. 253, p. 113 595, 2019.

[35] W. Li *et al.*, "Real-time energy disaggregation at substations with behind-the-meter solar generation," *IEEE Transactions on Power Systems*, vol. 36, no. 3, pp. 2023–2034, 2021.

[36] J. Lin, J. Ma, and J. Zhu, "A privacy-preserving federated learning method for probabilistic community-level behind-the-meter solar generation disaggregation," *IEEE Transactions on Smart Grid*, pp. 1–1, 2021. DOI: 10.1109/TSG.2021.3115904.

[37] L. Mauch *et al.*, "A novel dnn-hmm-based approach for extracting single loads from aggregate power signals," in *International Conference on Acoustics, Speech and Signal Processing (ICASSP)*, IEEE, 2016, pp. 2384–2388.

[38] B. Mirletz and D. Guittet, "Heuristic dispatch based on price signals for behind-the-meter PV-battery systems in the system advisor model," National Renewable Energy Laboratory, Tech. Rep., 2021. [Online]. Available: https://www.nrel.gov/docs/fy21osti/79575.pdf.

[39] H. Mohsenian-Rad *et al.*, "Guest editorial theory and application of pmus in power distribution systems," *IEEE Transactions on Smart Grid*, vol. 11, no. 1, pp. 723–725, 2020.

[40] B. Nate *et al.*, *System advisor model (sam) general description (version 2017.9.5)*, 2018.

[41] B. Nykvist and M. Nilsson, "Rapidly falling costs of battery packs for electric vehicles," *Nature Climate Change*, vol. 5, pp. 329–332, Mar. 2015. DOI: 10.1038/nclimate2564.

[42] OpenStreetMap contributors, *OpenStreetMap*, https://www.openstreetmap.org, 2017.

[43] F. Pedregosa *et al.*, "Scikit-learn: Machine learning in python," *Journal of Machine Learning Research*, vol. 12, no. Oct, pp. 2825–2830, 2011.

[44] U. T. Repository, *Smart* dataset*, http://traces.cs.umass.edu/index.php/Smart/Smart.

[45] P. Shaffery *et al.*, "Bayesian structural time series for behind-the-meter photovoltaic disaggregation," in *Innovative Smart Grid Technologies Conference*, IEEE, 2020, pp. 1–5.

[46] H. Shaker *et al.*, "A data-driven approach for estimating the power generation of invisible solar sites," *IEEE Transactions on Smart Grid*, vol. 7, no. 5, pp. 2466–2476, 2016.

[47] ——, "Estimating power generation of invisible solar sites using publicly available data," *IEEE Transactions on Smart Grid*, vol. 7, no. 5, pp. 2456–2465, 2016.

[48] X. Shi *et al.*, "Nonintrusive load monitoring in residential households with low-resolution data," *Applied Energy*, vol. 252, p. 113 283, 2019.

[49] S. Singh *et al.*, "Compressive non-intrusive load monitoring," in *Proc. 7th International Conference on Systems for Energy-Efficient Buildings, Cities, and Transportation*, ACM, 2020, pp. 290–293.

[50] Solcast, *Weather dataset*, https://toolkit.solcast.com.au/.

[51] F. Sossan *et al.*, "Unsupervised disaggregation of photovoltaic production from composite power flow measurements of heterogeneous prosumers," *IEEE Transactions on Industrial Informatics*, vol. 14, no. 9, pp. 3904–3913, 2018.

[52] C. D. G. Statistics, *Iou solar pv net energy metering (nem) interconnection data*, https://www.californiadgstats.ca.gov/downloads/.

[53] J. Stein, "The photovoltaic performance modeling collaborative (pvpmc)," in *38th Photovoltaic Specialists Conference*, IEEE, 2012, pp. 003 048–003 052.

[54] M. Tabone *et al.*, "Disaggregating solar generation behind individual meters in real time," in *Proc. 5th Conference on Systems for Built Environments*, ACM, 2018, pp. 43–52.

[55] B. Völker *et al.*, "Fired: A fully-labeled high-frequency electricity disaggregation dataset," in *Proc. 7th International Conference on Systems for Energy-Efficient Buildings, Cities, and Transportation*, ACM, 2020, pp. 294–297.

[56] E. Vrettos *et al.*, "Estimating pv power from aggregate power measurements within the distribution grid," *Journal of Renewable and Sustainable Energy*, vol. 11, no. 2, p. 023 707, 2019.

[57] S. Wang *et al.*, "Regional nonintrusive load monitoring for low voltage substations and distributed energy resources," *Applied Energy*, vol. 260, p. 114 225, 2020.

[58] M. Wytock and J. Z. Kolter, "Contextually supervised source separation with application to energy disaggregation," in *Proc. 28th AAAI Conference on Artificial Intelligence*, AAAI Press, 2014, pp. 486–492.

[59] J. Yan *et al.*, "Joint energy disaggregation of behind-the-meter PV and battery storage: A contextually supervised source separation approach," in *IEEE/IAS 57th Industrial and Commercial Power Systems Technical Conference*, 2021, pp. 1–9.

[60] Gu-yuan Lin *et al.*, "Applying power meters for appliance recognition on the electric panel," in *Proc. 5th Conference on Industrial Electronics and Applications*, IEEE, 2010, pp. 2254–2259.

[61] C. Zhang *et al.*, "Sequence-to-point learning with neural networks for non-intrusive load monitoring," in *AAAI*, 2018.